

**K-BEST SPHERE DETECTOR BASED RECEIVER
FOR MIMO NON-ORTHOGONAL MULTIPLE
ACCESS SYSTEMS**

Nawagamuwalage Niroshani Sriyanthi Ranaweera
(158485A)

Thesis submitted in partial fulfillment of the requirements for the degree Master of
Science in Telecommunications

Department of Electronic and Telecommunication Engineering

University of Moratuwa
Sri Lanka

2019

DECLARATION

I declare that this is my own work and this thesis does not incorporate without acknowledgement any material previously submitted for a Degree or Diploma in any other University or institute of higher learning and to the best of my knowledge and it does not contain any material previously published or written by another person except where the acknowledgement is made in the text.

Also, I hereby grant permission to University of Moratuwa, the non-exclusive right to reproduce and distribute my thesis, in whole or in part in print, electronic or other medium. I retain the right to use this content in whole or part in future works (such as articles or books).

N Sriyanthi Ranaweera
(signature of the Student)

The above candidate has carried out research for the Masters under our supervision.

Dr. K. C. B. Wavegedara,
Research supervisor,
Women's Campus,
Higher Colleges of Technology (HCT),
Ras Al Khaimah, UAE.

Dr. Tharaka Samarasinghe,
Research co-supervisor,
Senior Lecture,
Dept. of Electronic and Telecommunication Engineering,
University of Moratuwa.

ABSTRACT

K-Best Sphere Detector based Receiver for MIMO Non-Orthogonal Multiple Access Systems

Non-Orthogonal Multiple Access (NOMA) is a promising radio access technology, which improves the spectrum efficiency and system throughput considerably over conventional Orthogonal Multiple Access (OMA) techniques and also enables massive connectivity. NOMA is currently being considered extensively as a key enabling technology for 5G wireless networks. However, in NOMA, one of the key technical challenges is to develop efficient receivers due to the presence of Multiple-Access Interference (MAI) caused by non-orthogonal resource allocation. Minimum Mean Square Error (MMSE) based Successive Interference Cancellation (SIC) receivers have widely been discussed in the literature for power-domain NOMA systems. However MMSE detector is a linear detector with poor error performance. In this research, a K-Best sphere detector based SIC receiver is discussed for the downlink of power-domain MIMO-NOMA systems. The BER performance of the proposed receiver is investigated for different power allocation ratios and for different K values of the K-Best detector. Link level simulation results demonstrate that our proposed K-Best detector based receiver offers much superior performance over the MMSE-SIC based receiver.

Keywords : NOMA, SIC, MIMO

To my parents ...

ACKNOWLEDGEMENTS

First and foremost, I wish to express my heartfelt sincere gratitude to my research supervisor, Dr. K.C.B. Wavegedara, (Former Senior Lecturer, Department of Electronic and Telecommunication Engineering, university of Moratuwa). I am very much indebted to you sir, for all your assistance given to me during my research.

I would also like to thank my co-supervisor and the MSc coordinator Dr. Tharaka Samarasinghe (Senior Lecturer, Department of Electronic and Telecommunication Engineering) for the guidance and support provided me to complete my research.

On a more personal note, I am extremely indebted to my beloved parents and my dearest husband for being a constant source of inspiration, strength and encouragement throughout this endeavor.

Finally, I would like to extend my gratitude towards all the lecturers, my batch mates and all the others who helped me on this research.

TABLE OF CONTENTS

1	INTRODUCTION	1
1.1	Background	1
1.1.1	NOMA	2
1.1.2	OFDMA	8
1.2	Statement of the Problem	10
1.3	Objectives and Scope	11
1.4	Notation	12
1.5	Organization of the Thesis	12
2	LITERATURE REVIEW	13
2.1	Introduction	13
2.2	MIMO Detection Algorithms	13
2.2.1	ML Detector	15
2.2.2	Linear MMSE Detector	15
2.2.3	Sphere Detector	16
2.2.4	SIC Receivers	19
2.3	Receivers for NOMA-SISO and SIMO Systems	19
2.3.1	Summary	22
2.4	Receivers for NOMA-MIMO Systems	23
2.4.1	Summary	25
3	SYSTEM MODEL AND MATHEMATICAL FORMULATION	26
3.1	Introduction	26
3.2	System Model for NOMA in Single-Carrier MIMO	27
3.2.1	Joint Constellation	30
3.3	System Model for NOMA in MIMO-OFDMA Systems	31

3.3.1	Layer mapping	32
3.3.2	Pre-coding for Large Delay Cyclic Delay Diversity	33
3.3.3	OFDMA mapping	34
4	PROPOSED RECEIVER SCHEMES	35
4.1	Introduction	35
4.2	Proposed Receiver Structure for NOMA in Single-Carrier MIMO Systems . . .	35
4.2.1	MMSE Detector for Power Domain NOMA	37
4.2.2	K-Best Detector for Power Domain NOMA	37
4.3	Receiver for NOMA in MIMO-OFDMA Systems	38
5	SIMULATION RESULTS AND DISCUSSION	40
5.1	Preliminary Results	40
5.2	Assumptions and System Parameters	42
5.3	Results obtained for NOMA in Single-Carrier MIMO Systems	43
5.4	Results obtained for NOMA in MIMO-OFDMA Systems	48
6	CONCLUSION AND FURTHER RESEARCH	52
6.1	Conclusion	52
6.2	Suggestions for Further Research	53

LIST OF FIGURES

1.1	OFDMA sub-channels	8
2.1	Classification of MIMO detection algorithms	14
2.2	Tree search representation of 2x2 MIMO for QPSK	17
2.3	Symbol Level and Code Word Level SIC	19
3.1	Downlink Power Domain NOMA with SIC for 2x2 MIMO system	27
3.2	Transmitter of Single Carrier 2x2 MIMO DL system	27
3.3	Illustration of the Joint constellation	31
3.4	Fundamental block diagram of transmitter of the MIMO-NOMA-OFDMA system	32
3.5	Cyclic Delay Diversity	33
4.1	Proposed receiver for cell-center user	36
4.2	BER performance without considering joint modulation	38
4.3	Receiver for NOMA in MIMO-OFDMA systems	39
5.1	BER performance for 2x2 MIMO with QPSK	41
5.2	BER performance for 4x4 MIMO with BPSK	41
5.3	BER performance for 4x4 MIMO with QPSK	42
5.4	BER performance for 2x2 MIMO NOMA system	44
5.5	BER performance for different power levels with RS-1 and RS-3	45
5.6	BER variation with power ratio at $E_b/N_0=16$ dB	46
5.7	BER performance for different K values	47
5.8	BER performance by using QPSK for cell-edge user and 16-QAM for cell-center user	48
5.9	BER performance for 4x4 MIMO	49
5.10	BER performance for OFDMA system	50

5.11 BER performance for OFDMA with different power levels	51
5.12 BER performance for OFDMA with different K values	51

LIST OF TABLES

2.1	Summary of SD algorithms	18
2.2	Summary of SISO and SIMO detectors	22
2.3	Summary of MIMO detectors	25
3.1	QPSK modulation mapping	28
3.2	16-QAM modulation mapping	29
3.3	Transmission modes define in LTE	34
3.4	FFT length in LTE	34
4.1	Receiver Schemes Tested in the research	37
5.1	System parameters used in simulation	43

LIST OF ABBREVIATIONS

AWGN Additive White Gaussian Noise. 3

BER Bit Error Rate. 6

BLER Block Error Rate. 23

BS Base Station. 4

CCD Cyclic Delay Diversity. 33

CDMA Code Division Multiple Access. 1

CP Cyclic Prefix. 8

CSI Multiple Access Interference. 3

CWIC Code Word level SIC. 23

DL Down Link. 3

DoF Degree of Freedom. 20

ED Euclidean distance. 15

FDMA Frequency Division Multiple Access. 1

FFT Fast Fourier Transform. 8

IFFT Inverse Fast Fourier Transform. 8

IoT Internet of Things. 1

IR Increased Radius. 18

ISI Inter Symbol Interference. 3

LD Linear Detector. 15

LDS Low Density Spreading. 7

LTE Long Term Evolution. 2

MA Multiple Access. 1

MAI Multiple Access Interference. 2

MCS Modulation and Coding Schemes. 23

MIMO Multiple Input Multiple Output. 2

ML Maximum Likelihood. 10

MMSE Minimum Mean Square Error. 5

MUD Channel State Information. 3

MUSA Multi User Shared Access. 7

NOMA Non-Orthogonal Multiples Access. 1

OFDMA Ortogonal Frequency Division Multiple Access. 1

OMA Orthogonal Multiples Access. 1

PA Power Allocation. 6

PAPR Peak-to-Average Power Ratio. 9

PED Partial Euclidean distance. 16

QoS Quality of Service. 6

QRD QR Decomposition. 16

RB Resorce Block. 2

SCMA Sparse Code Multiple Access. 7

SD Sphere Detector. 16

SEE Schnorr Euchner Enumeration. 18

SIC Successive Interference Cancellation. 5

SIMO Single Input Multiple Output. 19

SISO Single Input Single Output. 13

SLIC Symbol level SIC. 23

SNR Signal to Noise Ratio. 20

TDMA Time Division Multiple Access. 1

TIM Topological Interference Management. 20

TM3 Transmission Mode 3. 23

UL Up Link. 3

Chapter 1

INTRODUCTION

1.1 Background

In the evolution of mobile communication systems, Multiple Access (MA) technology is one of the main distinguished technologies used to address the network demand with the available network resources. Depending on the MA technology used, efficiency of utilizing network resources, mainly the number of supported users and the expected user throughput are changed. For an example, 1G, 2G, 3G and 4G wireless communication systems use Frequency Division Multiple Access (FDMA), Time Division Multiple Access (TDMA), Code Division Multiple Access (CDMA) and Orthogonal Frequency Division Multiple Access (OFDMA) respectively, as their MA technology. The MA technologies can be broadly divided into two main categories.

1. Orthogonal Multiples Access (OMA)
2. Non-Orthogonal Multiple Access (NOMA)

The past generations of mobile communication systems used OMA technologies. In the OMA technologies, the wireless resources are orthogonally allocated to the multiple users in frequency, time or code domain in order to avoid or minimize inter-user interference. The number of supported users are limited by the number of available orthogonal resources in the OMA technologies. Further, even though the transmitted signals are orthogonal, received signals are non orthogonal due to dispersive channel [1] i.e. frequency selective channel.

Fast development of the Internet of Things (IoT) and the mobile internet targets to challenging requirements for the future 5G networks such as ten thousand times capacity of current network, hundred times new connected devices than 4G, 1 Gbps peak data rate, 100 Mbps data

rate at the cell edge and less than 1 ms latency [2]. Multiple Input Multiple Output (MIMO) systems and NOMA are among the key enabling technologies to provide the future network demand. Recently NOMA has received a tremendous attention as a promising radio access technology which allows multiple users to share the network resources simultaneously. As an example in OFDMA, users' signals are orthogonal in the frequency and/or time domains. One resource block (RB), which occupies 180 kHz in 4G Long Term Evolution (LTE) standard cannot be allocated to more than one user. However combining OFDMA with NOMA technology, one RB can be allocated to two or more users simultaneously [3]. Hence in NOMA, the number of supported users are not limited to the availability of orthogonal resource units. There are two main categories of NOMA.

1. Power Domain NOMA

2. Code Domain NOMA

The near far effect of the cell-center user and the cell-edge user is considered for the transmit power allocation and to detect the received signals in power domain NOMA. There is a key difference compared to the conventional CDMA in 3G and Code Domain NOMA. That is the spreading sequences are restricted to the sparse sequences or the non-orthogonal low cross-correlation sequences in NOMA [1, 4]. Further, CDMA technology is basically designed to separate the users by exploiting the differences among their spreading codes. However NOMA enables users to use exactly the same code simultaneously. As a result, chip rate of CDMA should be much higher than the information rate. As an example supporting a data rate of 10 Gbps may require a chip rate of a few hundred Gbps which is difficult to realize with practical hardware [5].

A more comprehensive description about NOMA is included in the Subsection 1.1.1. Due to the non orthogonality of the resource allocation in NOMA, Multiple Access Interference (MAI) is increased and one of the key technical challenge in NOMA is designing efficient receivers.

1.1.1 NOMA

As stated before 1G to 4G cellular mobile communication systems were mainly developed using OMA approaches, which avoid intra-cell interference and simplify air interface design. However OMA technologies have no ability to handle the inter-cell interference. Therefore

physical parameters and logical parameters of cells should be properly planned to minimize the inter-cell interference. [1].

The concept of NOMA has been proposed to support more users than the number of available orthogonal time, frequency or code domain resources, so that the future network demand can be fulfilled. The main idea of NOMA is to support non-orthogonal resource allocation among the users and hence increase the systems throughput and the spectral efficiency. However the receiver complexity will be increased because the receiver should be capable of separating the non-orthogonal signals, i.e., the overlapping signals in time, frequency or code domain).

NOMA has both benefits and challenges compared to OMA. The main challenge is dealing with inter-user interference due to non-orthogonal resource allocation and hence increasing receiver complexity. We are addressing the same challenge in this research. It can be seen that if the challenges can be properly addressed, NOMA possesses some good advantages over OMA which are described below.

Advantages of NOMA over OMA

- **Improved spectral efficiency and system throughput**

As discussed in [1], both OMA and NOMA achieve the channel capacity. However NOMA is capable of providing more user fairness in uplink (UL) of NOMA systems. Further, the capacity limit of NOMA is much higher than that of OMA in the downlink (DL) of Additive White Gaussian Noise (AWGN) channels. In the case of multi-path fading channels experiencing inter-symbol-interference (ISI), only the OMA can achieve the channel capacity in DL. NOMA relying on Multi User Detection (MUD) is optimal and OMA is sub optimal, if the Channel State Information (CSI) is known at the DL receiver.

- **Massive connectivity**

The number of simultaneous users are not limited by the availability of the orthogonal resources in NOMA. Therefore, NOMA is capable of significantly increasing the number of simultaneous connections [1]. Therefore it has the potential to support massive connectivity. This is a very important feature for 5G. With the evolution of IoT, hundreds of sensors will be connected to the internet simultaneously in the sensor net-

works installed for smart agriculture, smart cities and vehicular communications. These sensors may require only a few kilobytes of data to be transmitted but the simultaneous connectivity is very important. NOMA is capable of catering for such a network requirement. However, the number of simultaneous connections are limited with the NOMA technology used and the receiver capabilities.

- **Low transmission latency and signaling overhead**

In the conventional OMA systems, first a user needs to send a scheduling request to the base station (BS) which is known as access-grant request. If the request is received by the BS, it schedules the user's UL transmission by sending a clear-to-send signal in the DL channel. The transmission latency and signaling overhead is considerably high in this process and it's not acceptable in 5G. In LTE, access grant process takes about 15.5ms however the 5G latency requirement is less than 1ms. Some of the UL NOMA technologies do not require dynamic scheduling and hence reduce the latency and signaling overhead.

- **Relaxed channel feedback**

Since the CSI feedback is only used for power allocation, the channel feedback requirement will be relaxed in power domain NOMA, . Therefore there is no requirement for accurate instantaneous CSI knowledge. If the channel is not changing rapidly, even a limited accuracy out dated channel feedback will not be severely affected the system performance [1]

- **No need to increase number of transmit antennas**

It is not required to increase the number of antennas specifically for NOMA implementation. This feature is quite important from the perspective of the cost and the space limitations of small cells and macro cell deployments in nowadays practical networks. However, NOMA can be used with beam forming and MIMO to introduce the diversity and to increase the system throughput [4].

- **Compatibility with OFDMA and SC-FDMA**

NOMA can be easily combined with OFDMA for DL and SC-FDMA for UL to adjust with LTE releases [4].

Considering the above advantages, NOMA is considered as a very promising Radio Access Technology for 5G and hence NOMA is actively being investigated. Most of the existing research papers on NOMA [4, 6, 7] focus on the power domain NOMA. Code domain NOMA schemes are briefly introduced in [8, 5].

Power Domain NOMA

In power domain multiplexing, multiple users share the same time, frequency resources and the power level is used to separate the different user signals. Then the multiple users are detected at the receiver by MUD algorithm such as Successive Interference Cancellation (SIC). Near far effect is utilized for power allocation and the signal separation. At the transmitter, different signals generated by different users are combined after classic channel coding, modulation and power allocation. In this way, the spectral efficiency can be enhanced but the complexity of the receiver is increased compared to the conventional OMA.

More specifically, if we consider a two user scenario for DL, where one user is near to the base station (near user/cell-center user) and the other one is at the cell edge (far user/cell-edge user). The cell-center user is having a better channel condition than the cell-edge. Therefore the cell-edge user is allocated with more power than the cell-center user. Then the cell-edge user receives only its desired signal however the cell-center user receives both the signals. The cell-edge user signal is the stronger signal received to the cell-center user. Therefore the cell-edge user can use a conventional receiver like Minimum Mean Square Error (MMSE). However MUD is required for the cell-center user. Since the cell-edge user signal is stronger at the cell-center user, cell-center user will first detect the cell-edge user signal and then its' interference is removed from the received signal to detect the desired cell-center user signal, i.e., SIC.

If there are several users, this process have to continue starting from the nearest user or the user having the best channel condition. The far users need to wait till the near users' signals are detected and interference being canceled. Therefore, there should be an upper bound on the number of users relying on SIC and more advance MIMO detection technologies should be used for serving more users . This is a bottle neck of using SIC for NOMA detection

Multi-user power allocation, SIC error propagation and user mobility are main concerns on power domain NOMA and discussed in [9]. Combination of power domain NOMA with MIMO can be used to further improve the system throughput and the spectral efficiency.

Power Allocation

Power allocation is very important in NOMA because the benefits of NOMA depend on the resource allocation, such as power allocation and channel assignment. Therefore there are many research papers which discuss about power allocation and [10, 11, 12] are some of them where different power allocation strategies for NOMA are presented.

According to [11], two Power Allocation (PA) strategies for power domain NOMA are proposed. The first strategy is based on CSI experienced by NOMA users. The proposed algorithm is assigned power to the users which is inversely proportional to the CSI of the users. The second strategy is based on predefined Quality of Service (QoS) per NOMA user. In this method the power is allocated to achieve predefined QoS for particular users. The simulations have shown that the first PA strategy based on the CSI is capable of achieving around 30% improvement for overall system throughput.

Optimum PA is discussed in [12] where the optimal power allocation is analytically characterized with given channel assignment compared to multiple channels under different performance criteria such as the maximum fairness, weighted sum rate maximization, energy efficiency maximization with weights or QoS constraints and sum rate maximization with QoS constraints in NOMA systems.

In [10], three PA methods are discussed. One of them is the simple predefined fixed power allocation and another two are based on constraints. One is to achieve a predefined QoS requirement and the next one to achieve more dynamic QoS requirement. This says that NOMA is having better performance than conventional MIMO-OMA, even with simple selection of power allocation coefficients.

In this research we consider the simple fixed power allocation ratio between the cell-center user and the cell-edge user, and compare the Bit Error Rate (BER) performance with different power allocation ratios.

Code Domain NOMA

Code domain multiplexing is extended from classic CDMA in 3G where the users share the same time and frequency resources. The users are assigned a user specific spreading code to identify the different users. However not like CDMA, spreading sequences are non-orthogonal low cross-correlation sequences in NOMA [1, 4]. There are few types of code domain NOMA schemes discussed in the literature.

- **Low Density Spreading CDMA**

Low Density Spreading (LDS) CDMA use sparse spreading sequences where conventional CDMA uses dense spreading sequence[13] to reduce the interference at each chip. Therefore LDS-CDMA can improve the system performance by using LDS sequences for CDMA. This is the only difference in LDS-CDMA compared to classic CDMA. Interference can be decreased among multiple users with proper planning of spreading sequence and overloading also achieved in LDS-CDMA.

- **Low Density Spreading OFDMA**

This is a combination of LDS-CDMA and OFDMA which is specially designed to overcome the multipath fading issue. Transmitted symbols are first mapped to a certain LDS sequence and transmitted over OFDMA sub carriers in LSD-OFDMA.

- **Sparse Code Multiple Access**

This is an improved version of LDS-CDMA. Sparse Code Multiple Access (SCMA) is about mapping different bit streams to different sparse code words. Main difference between LDS-CDMA and SCMA is the shaping gain. The 'shaping gain' is defined as the average symbol energy when the shape of a constellation is changed [14]. If the constellation is closed to a sphere, shaping gain is having higher value [14].

- **Multi User Shared Access**

In UL Multi User Shared Access (MUSA), symbols of each user are spread by a spreading sequence which should have low cross-correlation. Each user randomly select one code from a pool of spreading sequences. Different spreading sequences may also be used for different symbols of a same user, which can further improve the performance through interference averaging [15].

Users are separated into groups in DL MUSA. In each group, different user symbols are mapped to different constellations in a way that Gray mapping can be ensured in the joint constellation of combined signals. The modulation level and the power level of each user is defined the joint constellation.

1.1.2 OFDMA

OFDMA is the MA technique used for radio transmission and reception in LTE. OFDMA is a powerful way to minimize the problems of fading and ISI. If the channel response is larger than the duration of the pulse, ISI may occur in time domain. In frequency domain this leads to frequency selective fading but if the total bandwidth is split into several sub bands, each band undergoes flat fading and ISI can be eliminated. Therefore, in frequency domain OFDM divides the wide band channel into small sub-channels which are overlapped with adjacent sub-channels. These sub-channels are orthogonal hence there is no interference among sub-channels at the sampling point. Implementation of Cyclic Prefix (CP) can undermine the ISI caused by delay spread. The concept of OFDMA is shown in Fig 1.1.

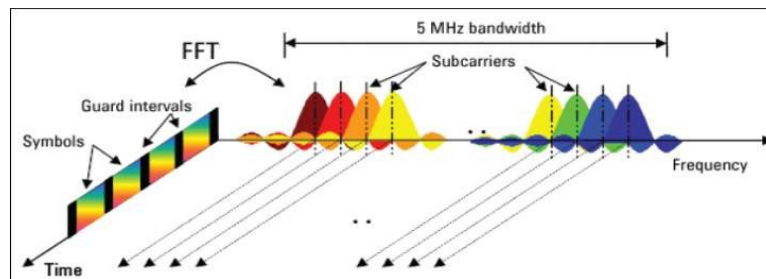


Figure 1.1: OFDMA sub-channels

[16]

The benefits of OFDMA can be summarized as,

- Dividing the large bandwidth into small sub carriers to minimize the frequency-selective fading.
- It can be against ISI, so it is suitable for high-speed data transmission in multi-path environment.
- Spectrum efficiency is maximized because of the orthogonality between sub carriers, adjacent sub channels can be overlap.
- Modulation and demodulation can be achieved by Inverse Fast Fourier Transform (IFFT) and Fast Fourier Transform (FFT). Hence calculation is efficient and simple.
- It can achieve the different UL and DL transmission data rate by using different number of sub-channels.

- It can take full advantage of high SNR sub channels to increase system throughput by dynamic sub channel allocation.

However there are few limitations of OFDMA as well.

- Sensitive to frequency deviation: Frequency shift occurred in transmission process (such as Doppler Shift) or the frequency difference between a receiver local oscillator and the carrier frequency of transmitter would undermine the orthogonality between sub carriers of OFDM system, leading to inter-channel signal interference.
- High Peak-to-Average Power Ratio (PAPR): The output of OFDM modulation is the superposition of multiple sub-channels. If the signal phases in multiple sub-channels are same at a certain time, superimposed signal instantaneous power will be far greater than the signal average power, resulting in a high PAPR. High PAPR not only brings higher requirements on transmitter Power Amplifier linearity, but also reduces the amplifier efficiency.

OFDMA is used not only for LTE but also for several other radio communication systems as follows.

- IEEE 802.11 versions a, g and n.
- WiMAX (IEEE 802.16).
- Digital television.
- Radio broadcasting.

1.2 Statement of the Problem

Receiver design is one of the main challenges in NOMA due to MAI. Use of SIC receivers for power domain NOMA has been addressed in many research papers [6, 7, 17]. Power domain NOMA is widely discussed than code domain NOMA because it is suitable for both the UL and the DL, efficiently utilize the power available at the BS or UE, minimize intra-cell interference and can be combined with MIMO to further increase the spectral efficiency.

In SIC receivers used in power domain NOMA, the interfering user, i.e. the cell-edge user signal is first detected and its interference is removed from the received signal of cell-center user to detect the cell-center user signal. Therefore the accuracy of detection of the interfering user affects the accuracy of the desired user detection. Otherwise the errors are propagated from user to user in multi user scenario.

The MMSE based SIC receivers for the cell-edge user detection at the cell-center user were widely discussed in the literature. Even though, the MMSE receivers are linear receivers with low complexity, the detection performance significantly degrades with the interference. Optimal signal detection is achieved using Maximum Likelihood (ML) detector. However the complexity of ML detectors exponentially increases with the modulation order and the number of transmit antennas. Therefore a sub optimal solution may be preferred which offers improved trade-off between complexity and performance.

1.3 Objectives and Scope

The main objective of this research study is to develop an efficient receiver for MIMO-NOMA-OFDMA systems which offers improved trade-off between the error performance and the complexity. The specific objectives are summarized as follows :

1. To carry out an extensive literature survey on NOMA schemes and candidate receivers.
2. To develop a computationally efficient receiver for MIMO-NOMA-OFDMA systems which offers improved trade-off between complexity and performance.
3. To implement a MIMO-NOMA-OFDMA system including the proposed receiver in MATLAB.
4. To investigate the error performance and limitations of the proposed receiver through simulations.
5. To compare the performance with existing receivers and propose further improvements.

The scope of the research is limited to propose a K-best sphere detector based receiver for the DL of MIMO Power Domain NOMA in single carrier systems and OFDMA systems. The error performance and the complexity of K-best sphere detector based receivers for MIMO-OFDMA systems over MMSE receiver and ML receiver are discussed in [18, 19, 20, 21].

1.4 Notation

Throughout this thesis we represent vectors in bold lower-case letters, and matrices in bold upper-case letters. $E\{\cdot\}$, $V\{\cdot\}$, $Cov\{\cdot\}$ stand for the expected value, variance and covariance operators respectively; $(\cdot)^T$, $(\cdot)^*$, and $(\cdot)^H$ denote the transpose, complex conjugate (component-wise), and Hermitian transpose operations, respectively.

1.5 Organization of the Thesis

Organization of this thesis is as follows. Literature review is exclusively covered in the next chapter. The literature review is presented under three subsections: MIMO detection, receivers for NOMA in SISO systems and receivers for NOMA with MIMO systems. Chapter 3 discusses the system model for MIMO-NOMA in both single carrier systems and NOMA-OFDMA systems. Mathematical formulation of a MIMO-NOMA-OFDMA system is presented in Chapter 4. In Chapter 5 we present the simulation results for proposed receiver for both single carrier and multi carrier systems. Finally we conclude the thesis with conclusion and suggestions for future research in Chapter 6.

Chapter 2

LITERATURE REVIEW

2.1 Introduction

In this chapter we mainly focus on the receivers design for the downlink of NOMA systems. The literature survey is extended to identify the receivers designed for both Single Input Single Output (SISO) and MIMO scenarios because the spectral efficiency and the system throughput can be considerably increased by combining NOMA with MIMO. Both the advantages and the limitations of different algorithms are studied during the literature review.

Literature review is organized covering following three main topics:

1. MIMO Detection Algorithms.
2. Receivers for NOMA-SISO Systems.
3. Receivers for NOMA-MIMO Systems.

2.2 MIMO Detection Algorithms

MIMO is a very promising technology for reliable data transmission and to provide high spectral efficiency. Usage of multiple antennas at both the transmitter and the receiver is capable of providing high data rate and to improve the transmission quality without increasing the transmit power and expanding the frequency spectrum. A linear superposition of the transmitted signals are observed at the receiver.

Optimal solution based on performance for MIMO detection is the ML detection and there are several sub optimal detection algorithms such as linear detection, interference cancellation detection and tree search based detection. MIMO detection algorithms can be broadly classified

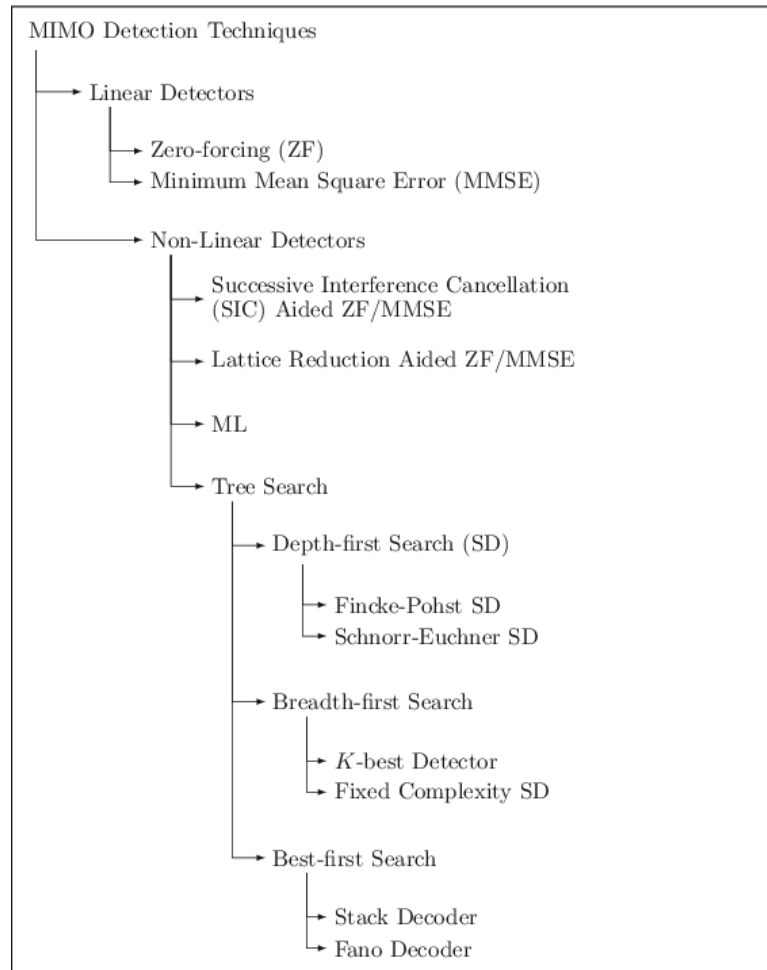


Figure 2.1: Classification of MIMO detection algorithms [22]

into two categories as linear detectors and non-linear detectors. Non-linear detectors can be classified according to Fig 2.1.

In this section we discuss ML detector and K-best sphere detector which is a sub optimal solution for ML detector and the linear MMSE detector. All these detectors have associated advantages and limitations with them.

2.2.1 ML Detector

The optimum hard-decision MIMO detector is the ML detector. It uses an exhaustive search to find the transmitted vector \mathbf{x} from the received symbols among $2^{l \times n_t}$ possible symbol combinations, where l is the number of bits per symbol and n_t is the number of transmitted antennas. Assuming an AWGN channel and the symbol vectors are equiprobable, the optimal ML solution can be derived as (2.1).

$$\mathbf{s}_{ML} = \arg \min_{\mathbf{x} \in 2^{l n_t}} \|\mathbf{y} - \mathbf{H}\mathbf{x}\|^2, \quad (2.1)$$

where \mathbf{H} is the $n_r \times n_t$ channel matrix, n_r is the number of received antennas, n_t is the number of transmitted antennas and \mathbf{y} is the received signal vector. The ML solution is based on finding the smallest Euclidean distance (ED) between the received symbol vector \mathbf{y} and each possible transmitted vectors. In the uncoded MIMO systems, ML detector provides the optimal performance but complexity of ML detector is exponentially increases with respect to the number of transmit antennas and the size of signal constellation. Therefore using ML detector is not feasible with higher number of transmit antennas and with higher order modulations.

2.2.2 Linear MMSE Detector

The Linear Detector (LD) or equalizer, basically uses a filtering matrix \mathbf{G}_{LD} to remove the impact of MIMO channel matrix. Filtering matrix which is constructed using Minimum Mean Squared Error criteria is known as MMSE detector.

The filtering matrix \mathbf{G}_{MMSE} is given in [23].

$$\mathbf{G}_{MMSE} = \arg \min_G E\{\|\mathbf{G}\mathbf{y} - \mathbf{x}\|\}, \quad (2.2)$$

where \mathbf{y} is the received symbol vector and \mathbf{x} is the transmitted symbol vector. Using the principle of orthogonality between the received vector and the noise vector:

$E\{(\mathbf{G}_{MMSE}\mathbf{y} - \mathbf{x})\mathbf{y}^H\}=0$, \mathbf{G}_{MMSE} can be computed as (2.3).

$$\mathbf{G}_{MMSE} = \left(\mathbf{H}^H \mathbf{H} + \frac{\sigma_n^2}{\sigma_x^2} \mathbf{I}_{n_t} \right)^{-1} \mathbf{H}^H, \quad (2.3)$$

where σ_x^2 and σ_n^2 are the variance of the transmitted vector and noise vector respectively.

Linear detectors having low computational complexity but those are not capable to reach the diversity order of the ML detector because of the independent detection of symbols [23].

2.2.3 Sphere Detector

Sphere Detector (SD) generate the ML solution with reduced complexity than the ML detectors [24]. Sphere detector limits the search space to the points which lie inside a n_r dimensional hyper-sphere $S(\mathbf{y}, \sqrt{c_0})$ centered at \mathbf{y} , where n_r is the number of received antennas and c_0 is the square of the radius. The condition is written as (2.4) according to [25].

$$\|\mathbf{y} - \mathbf{H}\mathbf{x}\|^2 \leq c_0. \quad (2.4)$$

The channel matrix \mathbf{H} can be decomposed by QR Decomposition (QRD) and (2.4) can be derived as follows:

$$\|\mathbf{y} - \mathbf{Q}\mathbf{R}\mathbf{x}\|^2 \leq c_0. \quad (2.5)$$

Multiplying both the sides of (2.5) by \mathbf{Q}^H ,

$$\|\mathbf{Q}^H\mathbf{y} - \mathbf{R}\mathbf{x}\|^2 \leq c_0, \quad (2.6)$$

$$\|\tilde{\mathbf{y}} - \mathbf{R}\mathbf{x}\|^2 \leq c_0, \quad (2.7)$$

where $\mathbf{R} \in \mathbb{R}^{n_t \times n_t}$ is an upper triangular matrix with positive diagonal elements and $\mathbf{Q} \in \mathbb{R}^{n_r \times n_t}$ is an orthogonal matrix and $\tilde{\mathbf{y}} = \mathbf{Q}^H\mathbf{y}$. Using the triangular nature of \mathbf{R} , the Euclidean distance matrix in (2.7) can be recursively evaluated through the accumulated Partial Euclidean Distance (PED) d_m , where $d_{n_t} + 1 = 0$ as (2.8).

$$d_m = d_{m+1} + |\tilde{\mathbf{y}} - \sum_{j=m}^{n_t} \mathbf{R}_{m,j}\mathbf{x}_j|^2, \quad (2.8)$$

where $m = n_t, \dots, 1$.

Calculating the PED can be illustrated by a tree with number of levels equals to $n_t + 1$ as illustrated in Fig 2.2, where level m corresponds to the m^{th} transmit antenna and the number of child nodes at a given node is equal to the size of the constellation $|\Omega|$. As an example, for 2x2 MIMO system with QPSK modulation, the corresponding tree is having three layers including the root layer and four child nodes for each parent node. The tree-search starts at the root level and the child node at level n_t corresponding to the symbols transmitted by the n_t^{th} antenna. The PED d_{n_t} in (2.8) is then computed. If $d_{n_t} - 1$ respects the sphere radius constraint c_0 , the search continues at level $n_t - 1$ and steps down the tree at level m until it finds a valid leaf node at level 1.

There are three main search types in tree search algorithms. Depth first search, Breadth first search and Matrix first search [20]. Based on the searching method there are different SD algorithms [19].

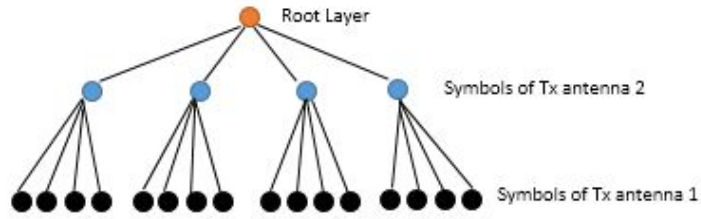


Figure 2.2: Tree search representation of 2x2 MIMO for QPSK

- **K-Best Sphere Detector**

K-Best algorithm is based on the breadth first search strategy, i.e., the search starts from the root layer and continue one level at a time by calculating the PEDs of the admissible nodes and selecting the K number of best candidates to the next level, i.e., K number of candidates with minimum PED. Then the search is continued with the selected K partial candidates.

K-Best Algorithm according to [20]

Preprocessing:

Input: $\mathbf{Q}, \mathbf{R}, \mathbf{y}, c_0, K, P$ (modulation used P-QAM)

Calculate: $\tilde{\mathbf{y}}$

Algorithm

1. Start from the root layer with empty candidate set
2. Partial candidate set is denoted by \mathbf{x}_{m+1}^{nt} .
 - (a) Identify all admissible candidate child nodes x_m with given c_0 and calculate the PEDs $d(\mathbf{x}_m^{nt})$
 - (b) Store the candidates and their PEDs to a temporary stack memory
3. Sort the partial candidates according to their PEDs and save the K number of candidates having lowest PEDs and the PEDs to the final list stack memory.
4. If the K saved candidates are leaf nodes, stop the algorithm. Output is the saved candidates and their ED. Otherwise, continue to step 2 with the saved candidates.

- **SEE Sphere Detector**

Schnorr Euchner Enumeration (SEE) SD algorithm is based on depth first search algorithm. The search continues with the next best admissible node defined by SEE [20]. Either if it reaches to leaf level or exceed the sphere radius c_0 , the search will stop. This algorithm gives the candidate with lowest EDs however the throughput is variable .

- **IR Sphere Detector**

The Increased Radius (IR) algorithm is based on metric first search strategy. It is optimal based on the number of visited nodes. The search proceeds by calculating one branch extension at a time and stores the partial candidate to a stack memory. search continue with the lowest PED and out put is the candidate with lowest ED.

Table 2.1 summarizes the above mentioned SD algorithms.

Algorithm	K-Best SD	SEE SD	IR SD
Search Method	Breadth First Search	Depth First Search	Metric First Search
Throughput	Fixed	Variable	Variable
Output	Not necessarily the candidate with lowest ED	Candidate with lowest ED	Candidate with lowest ED
Implementation	Good performance in limited search hence feasible to implement.	Poor performance in limited search. Hardware implementation is difficult.	Good performance in limited search hence feasible to implement.

Table 2.1: Summary of SD algorithms

2.2.4 SIC Receivers

The basic idea of interference cancellation detection is recursively detecting the transmitted symbols to cancel the interference. In SIC, the strongest signal is detected first and its interference is cancelled from each received signal rather than jointly detecting signals. After that the second strongest signal is detected and its' interference is cancelled from the remaining signals and so on. This procedure is repeated until the detection of all the users are completed. It assumes the the interference from the cell-edge user is completely removed at the receiver of cell-center user in ideal SIC receiver. It provides an upper bound for DL NOMA receiver [7].

However in reality interference from cell-edge user can not be totally removed from the cell-center user due to less accurate symbol detection. Therefore SIC receivers suffer from error propagation issue. There are two types of SIC receivers, symbol level and code word level SIC receivers. Channel decoding is not involved in symbol level SIC. In the code word level SIC receivers interfering signal is detected, demodulated, decoded and then re-encoded and modulated to cancel the interference according to Fig. 2.3. Therefore code word level SIC outperforms the symbol level SIC receiver [7, 6, 4] with increased complexity and delay due to channel decoding and re-encoding.

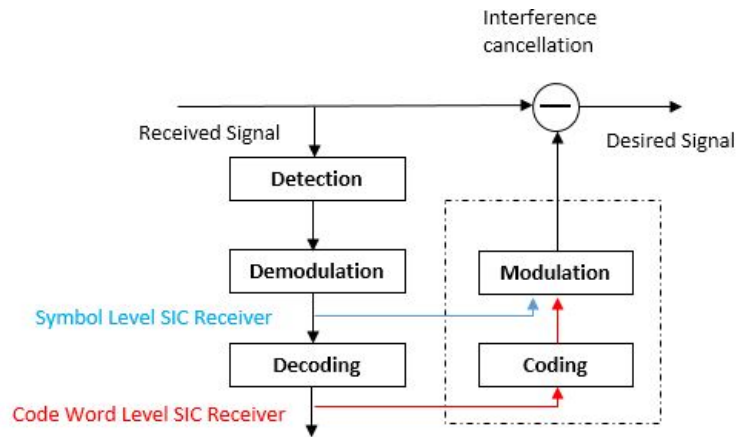


Figure 2.3: Symbol Level and Code Word Level SIC

2.3 Receivers for NOMA-SISO and SIMO Systems

In this section, receivers discussed for NOMA SISO systems and Single Input Multiple Output (SIMO) systems are discussed.

In [26], a hybrid Topological Interference Management (TIM) NOMA scheme in SISO system for K -user cells are discussed. There are T groups of users, and $1/T$ Degree of Freedom (DoF) is achieved for each user. By combining users in the power domain, they introduce a decoding process with two stages such as managing "inter-group" interference based on the TIM principles and "intra-group" interference based on SIC. They concluded for high Signal to Noise Ratio (SNR) values the hybrid scheme can improve the sum rate by at least 100% when compared to TDMA.

In Fair-NOMA, each mobile user is provided with its share of the transmit power to guaranteed its capacity which is always similar or higher than to the capacity of OMA. According to [27] the Fair-NOMA approach is applied to the pairing a near base station user and a cell edge user. SIC is used for signal detection. After that new method is compared to fixed-power NOMA with user pairing. their conclusion was the capacity can be improved for each user even with less transmit power than OMA.

Decoding time for DL NOMA with SIC is discussed in [28]. SIC depend on decoding and subtracting the signals in sequence until it reaches its desired signal. The decoding order at each User Equipment (UE) should match with the interference cancellation sequence. If there is a mismatch, UEs will not obtain their signals. However, this will increase the processing timer. They identified that the time for decoding operation varies according to the order of UE connected to the network that is the distance to the UE.

According to [7], MMSE based SIC receiver performances are evaluated with Log Likelihood Ratio (LLR) calculation based receiver for SIMO system using link level simulations. Furthermore, a novel transmission and receiving scheme is proposed for DL NOMA. At the transmitter side joint modulation is applied to signals of different users for achieving Gray mapping of the combined signal. LLR calculation method is used for receiver to directly decode the desired signal. Therefore complexity and decoding time is reduced at receiver side.

According to [29], NOMA schemes are classified into four categories: scrambling-based NOMA, spreading-based NOMA, coding-based NOMA, and interleaving-based NOMA. They summarize the transceiver block diagram of each category, and provide information of basic principles, key features, and transmission-reception algorithms of all NOMA schemes. MMSE-SIC receiver is discussed for scrambling-based NOMA, Minimum Mean Square Error with Parallel Interference Cancellation (MMSE-PIC) receiver is used to decode spreading-based NOMA, the Message Passing Algorithm (MPA) detector is implemented for coding-

based NOMA and MMSE-PIC is used for interleaving-based NOMA. According to their results, coding-based and spreading-based NOMA schemes have advantages in bigger connectivity and robustness.

2.3.1 Summary

A summary of different receivers for SISO and SIMO systems is presented in Table 2.2.

Name of the research paper	Decoder	Year	Remarks
A hybrid TIM-NOMA scheme for the SISO broadcast channel	MMSE-SIC	2015	For high SNR values the hybrid NOMA scheme can improve the sum rate by at least 100% when compared to TDMA
A fair power allocation approach to NOMA in multiuser SISO systems	MMSE-SIC	2017	Fair-NOMA can always improve the capacity for each user compared to OMA
NOMA with imperfect SIC implementation	MMSE-SIC	2017	Decoding time for Downlink NOMA with SIC is discussed
Receiver design for downlink Non-Orthogonal Multiple Access (NOMA)	LLR calculation based receiver	2015	LLR calculation method is used to directly decode the desired signal without SIC processing
Comprehensive study and comparison on 5G NOMA schemes	MMSE-SIC, MMSE-PIC, MPA	2018	categories of NOMA schemes are discussed with receivers

Table 2.2: Summary of SISO and SIMO detectors

2.4 Receivers for NOMA-MIMO Systems

Our objective is to propose an efficient receiver for MIMO-NOMA system. Therefore special consideration was given to study the MIMO receivers already discussed in literature for NOMA and identify their performance and limitations.

In [6], the performance of MMSE based SIC receiver for DL NOMA with 2x2 open-loop MIMO is discussed. Power domain multiplexing is used as NOMA technology. In addition, they have compared different SIC receivers in terms of performance such as Code Word level SIC (CWIC), Symbol Level SIC (SLIC), and ideal SIC. Link-level simulations are done assuming LTE Transmission Mode 3 (TM3), under different transmit power allocation ratios, rank combinations, and Modulation and Coding Schemes (MCS). The simulation results concluded that the CWIC receiver having higher performance compared to SLIC and has almost the same performance compared to ideal SIC when p_1 is below 0.35, and the MCS of cell center UE and cell edge UE is 16QAM (coding rate $R = 0.49$) and QPSK (coding rate $R = 0.49$) respectively.

Usage of MMSE based CWIC receiver and SLIC receiver are discussed in [4]. Performance of SLIC receiver is gradually decreased when the power allocation to the cell-edge user is decreased for power domain NOMA. Channel decoding is conducted in the signal detection for code word level SIC. Therefore the successful detection of cell-edge user improved significantly compared with SLIC. However channel decoding and re-encoding introduce additional computational complex and latency in CWIC.

According to [17], two low-complexity receiver techniques are proposed for DL NOMA (power domain) with SU-MIMO. For multi-stream signal, joint constellation is applied for detecting far user's signal at the cell center user. In this paper they have proposed limited search space method which limits the search nodes of sphere detector. Block Error Rate (BLER) performance and average time to detect the far user signal and near user signals are discussed in the paper for proposed receivers.

The computational complexity of multi user detection of proposed NOMA receivers are discussed in [15]. In power domain NOMA, MMSE based SIC is the main method for multi-user interference cancellation with complexity $\mathcal{O}(n^3)$, where n is the number of users. Similarly in code domain NOMA schemes, spreading sequences or code books should be known at the receiver to realize MUD. The complexity of the MPA-based receiver is $\mathcal{O}(|\mathcal{S}|^w)$ where w is the maximum number of nonzero signals superimposed on each chip or sub carrier and $|\mathcal{S}|$ denotes the cardinality of the signal constellation .

As per the literature review conducted for NOMA receivers, most of the papers have considered the MMSE-based SIC receivers. Their performance is comparatively poor but computational complexity is low and detection time also low. MMSE-based SIC performance is severely affected when the power allocation to the cell edge user is decreasing. When the far user signal detection is erroneous (BER is high) it will affect to the interference cancellation and signal detection of the near user. In the multi user scenario these errors will be propagated from a user to user. Therefore accuracy of interfering user detection is very important in SIC.

Similarly since we consider the DL signal detection, low processing complexity is also of very importance due to the fact that the processing power and power utilization is limited for UE and the detection algorithm should be capable of running on the UE side. Therefore the receiver should have good error performance and at the same time complexity should be handled by the UE.

2.4.1 Summary

Table 2.3 summarizes the different receivers for MIMO systems.

Name of the research paper	Decoder	Year	Remarks
Performance and design of SIC receiver for downlink NOMA with open-loop SU-MIMO	MMSE based SIC (Code Word level, Symbol level)	2015	Compared the performance of CWIC and SLSI receivers with Ideal SIC
Non-orthogonal multiple access (NOMA) for future downlink radio access of 5G	MMSE based SIC (Code Word level, Symbol level)	2015	Compared the performance of CWIC and SLSI
Limited search sphere decoder and adaptive detector for NOMA with SU-MIMO	Limited Search SD and MMSE-SIC	2016	Adaptive detector which can switches the detector according to MCS, power factor and estimated SNR
Non-orthogonal multiple access for 5G: solutions, challenges, opportunities, and future research trends	MMSE-SIC, ML, MPA-based Receiver	2015	Complexity of Different receiver algorithms are discussed

Table 2.3: Summary of MIMO detectors

Chapter 3

SYSTEM MODEL AND MATHEMATICAL FORMULATION

3.1 Introduction

In this chapter we present the system model and mathematical formulation for the power domain NOMA system for both single carrier MIMO and multi carrier MIMO. For the simplicity, we consider power domain NOMA with two users. One user is considered a cell-center user (near user) with better channel condition and the other user is considered the cell-edge user (far user) having poor channel condition. In the power domain NOMA, transmit signal power is allocated according to the channel condition of the users and power level is used to identify the different users as stated earlier. Fig. 3.1 illustrates the concept of DL NOMA SIC for a 2x2 MIMO system with one BS and two UEs. User 1 is the cell-center user and User 2 is the cell-edge user. The cell-edge user is allocated with more power compared to the cell-center user considering the channel condition.

Since the cell-center user is having lower power level compared to the cell-edge user, interference from the cell-center user is negligible at the cell-edge user. Hence the cell-edge user does not need an interference cancellation receiver and it is possible to directly decode its signals using a conventional receiver. However interference level is considerable at the cell-center user due to the transmit power of the cell-edge user. Therefore interference cancellation is required at the cell-center user as illustrated in Fig. 3.1.

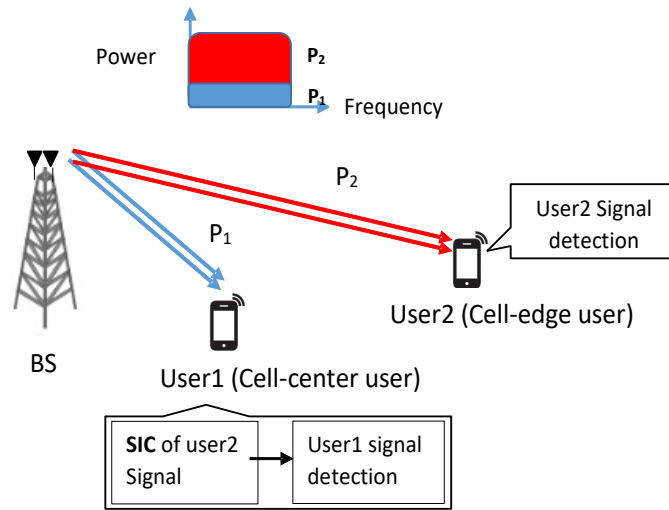


Figure 3.1: Downlink Power Domain NOMA with SIC for 2x2 MIMO system

3.2 System Model for NOMA in Single-Carrier MIMO

The system model for NOMA in Single Carrier MIMO scenario is discussed in this section. Channel coding is not considered. Information signals of the two users are separately modulated and pre-defined power level is allocated according to the channel condition. Then the two user signals are linearly superimposed to generate the transmitted signal according to the (3.1). The transmitter block diagram is shown in Fig. 3.2.

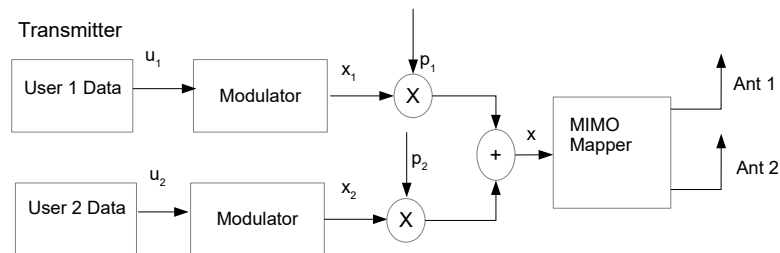


Figure 3.2: Transmitter of Single Carrier 2x2 MIMO DL system

$u_{i,j}$ represents the information bits of User 1 and User 2, where $u_{i,j} \in (1, 0)$ and i represents the user ($i = 1, 2$) and $j = 1, \dots, N$ represents the length of information block, where $N = 2048$. In the Fig. 3.2, u_1 and u_2 denote $\mathbf{u}_{1,j}$ and $\mathbf{u}_{2,j}$.

$$u_1 = \mathbf{u}_{1,j} = [u_{1,1}, u_{1,2}, \dots, u_{1,N}],$$

$$u_2 = \mathbf{u}_{2,j} = [u_{2,1}, u_{2,2}, \dots, u_{2,N}].$$

Information bits are fed to the modulation mapper to generate the complex valued modulation symbols $\mathbf{x}_{i,j}$. Elements of $\mathbf{x}_{i,j}$ are independently selected from complex constellation \mathcal{S}_i with l_i bits per symbol, where $x_{i,j} \in \mathcal{S}_i$ and $|\mathcal{S}_i| = 2^{l_i} = M_i$; $\mathcal{S}_i \in [\mathcal{S}_{i,1}, \mathcal{S}_{i,2}, \dots, \mathcal{S}_{i,M_i}]$.

As an example, $l_i = 2$ for QPSK modulation and $l_i = 4$ for 16-QAM modulation. In this research we used two cases where both the users use QPSK modulation and cell-center user uses 16-QAM while cell-edge user uses QPSK modulation. When the cell-center user is having a better SNR, it is possible to use a higher modulation to get higher throughput compared to the cell-edge user.

Complex symbol constellation \mathcal{S} of QPSK and 16-QAM modulation schemes are defined as [30] and given in Table 3.1 and Table 3.2, respectively, where \mathbf{I} is the real component and \mathbf{Q} is the imaginary component of the complex symbol.

$b(i), b(i+1)$	\mathbf{I}	\mathbf{Q}
00	$1/\sqrt{2}$	$1/\sqrt{2}$
01	$-1/\sqrt{2}$	$1/\sqrt{2}$
10	$1/\sqrt{2}$	$-1/\sqrt{2}$
11	$-1/\sqrt{2}$	$-1/\sqrt{2}$

Table 3.1: QPSK modulation mapping

In Fig. 3.2, x_1 and x_2 represent the transmitted symbol vectors of user i ($i = 1, 2$), $E[|\mathbf{x}_{i,j}|^2 = 1]$ and p_i ($p_1 < p_2, p_1 + p_2 = 1$) represents the allocated transmit power ratio to user i

$$x_1 = \mathbf{x}_{1,j} = [x_{1,1}, x_{1,2}, \dots, x_{1,N/l_1}]$$

$$x_2 = \mathbf{x}_{2,j} = [x_{2,1}, x_{2,2}, \dots, x_{2,N/l_2}]$$

At the BS, transmitted signal vector \mathbf{x} is generated as follows [6]:

$$\mathbf{x} = \sqrt{p_1}\mathbf{x}_1 + \sqrt{p_2}\mathbf{x}_2 \quad (3.1)$$

$b(i),b(i+1),b(i+2),b(i+3)$	I	Q
0000	$1/\sqrt{10}$	$1/\sqrt{10}$
0001	$1/\sqrt{10}$	$3/\sqrt{10}$
0010	$3/\sqrt{10}$	$1/\sqrt{10}$
0011	$3/\sqrt{10}$	$3/\sqrt{10}$
0100	$1/\sqrt{10}$	$-1/\sqrt{10}$
0101	$1/\sqrt{10}$	$-3/\sqrt{10}$
0110	$3/\sqrt{10}$	$-1/\sqrt{10}$
0111	$3/\sqrt{10}$	$-3/\sqrt{10}$
1000	$-1/\sqrt{10}$	$1/\sqrt{10}$
1001	$-1/\sqrt{10}$	$3/\sqrt{10}$
1010	$-3/\sqrt{10}$	$1/\sqrt{10}$
1011	$-3/\sqrt{10}$	$3/\sqrt{10}$
1100	$-1/\sqrt{10}$	$-1/\sqrt{10}$
1101	$-1/\sqrt{10}$	$-3/\sqrt{10}$
1110	$-3/\sqrt{10}$	$-1/\sqrt{10}$
1111	$-3/\sqrt{10}$	$-3/\sqrt{10}$

Table 3.2: 16-QAM modulation mapping

The signal constellation of the transmitted signal is changed to a combination of two constellations an which is know as joint constellation . Join constellation is discussed in the Subsection 3.2.1

When the cell-center user signal is detected, signals of the cell-edge user is considered as interference. However, signal of the cell-edge user is stronger than that of the cell-center user. Therefore the signals of cell-edge user is detected first and its' interference is cancelled from the received signal similar to the existing approach [6] . Then, the desired signal is detected and demodulated. As stated earlier, the cell-edge user can detect its signal without SIC, assuming that the effect of the interference cause by the cell-center user may be insignificant. Therefore, we focus only on the receiver of the cell-center user. Proposed receiver is discussed in Chapter 4.

3.2.1 Joint Constellation

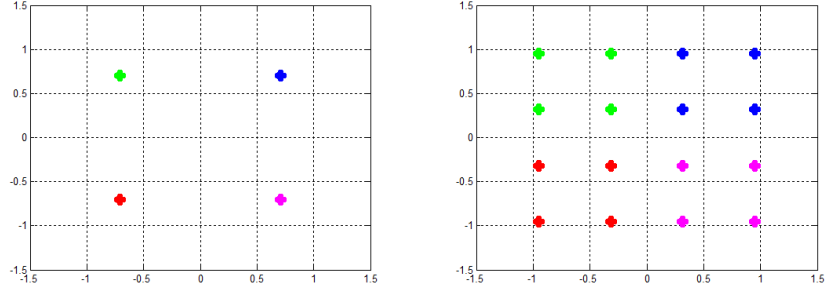
The shape of the constellation after joint modulation is determined by the modulation and the power ratio of each user. The size of the constellation is determined by the size of two constellations. Let the number of bits per symbol of the cell-center user be l_1 and the cell-edge user be l_2 , respectively. The size of the joint constellation is given by $2^{l_1+l_2}$. For an example, when both the users use QPSK modulation, $l_1 = l_2 = 2$ and then the size of the constellation is $2^{2+2} = 2^4 = 16$. Then the search tree has 16 branches for each parent node. Similarly if the cell-center user is using 16-QAM and the cell-edge user is using QPSK modulation, $l_1 = 4$ and $l_2 = 2$ and the size of joint constellation becomes $2^{4+2} = 2^6 = 64$.

Joint Constellation \mathcal{S}_{joint} is generated as (3.2).

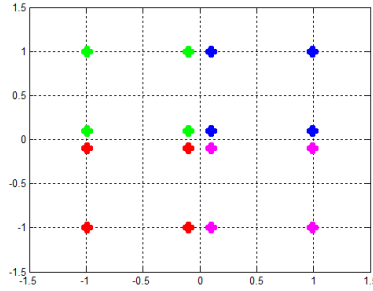
$$\mathcal{S}_{joint} = \sqrt{p_1} \times \mathcal{S}_1 + \sqrt{p_2} \times \mathcal{S}_2, \quad (3.2)$$

where p_1 and p_2 are power allocation ratios. \mathcal{S}_1 and \mathcal{S}_2 represent the symbol constellations of the users.

Fig 3.3 illustrates the joint constellation for different power levels when both the users use QPSK modulation.



(a) QPSK signal constellation for individual users (b) Joint constellation at the cell-center user for $p_1 : p_2 = 0.2 : 0.8$



(c) Joint constellation at the cell-center user for $p_1 : p_2 = 0.4 : 0.6$

Figure 3.3: Illustration of the Joint constellation

3.3 System Model for NOMA in MIMO-OFDMA Systems

The system model for MIMO-NOMA with multi carrier modulation is presented in this section. Here we explain about how to apply NOMA with OFDMA, where two users are allowed to share a single RB. The initial blocks of the transmitter is similar to the single carrier system. Different user signals are modulated separately and are combined with the predefined power allocation ratio and OFDMA mapping is applied before transmitting over the multiple antenna system.

The transmitter block diagram of the MIMO-NOMA-OFDMA system is shown in Fig.3.4. It is similar to the single carrier system in the initial stages but after the layer mapping transmitting signals are forwarded for OFDMA transmission.

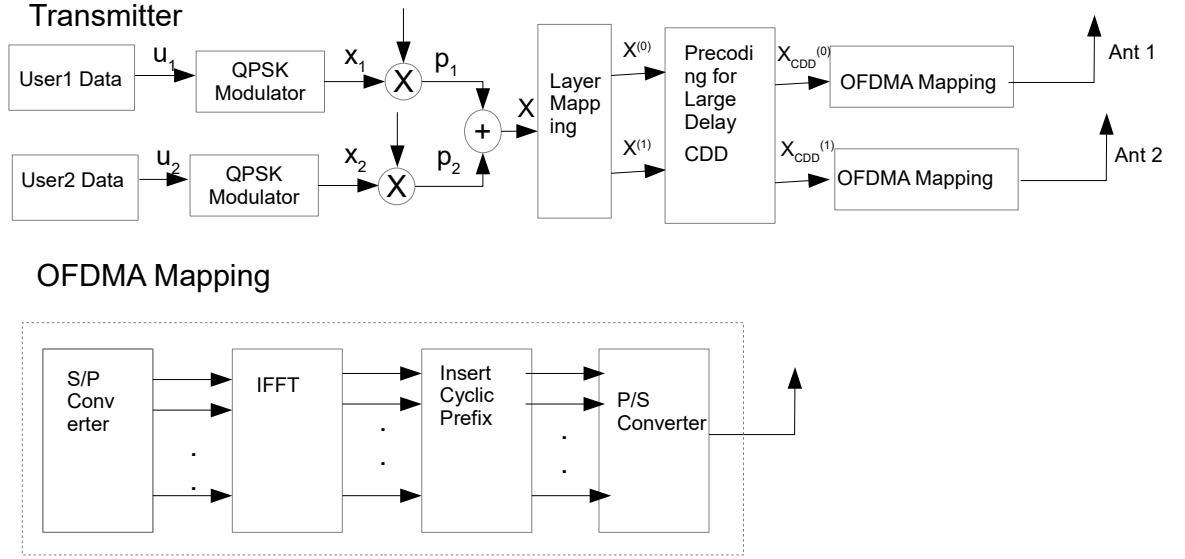


Figure 3.4: Fundamental block diagram of transmitter of the MIMO-NOMA-OFDMA system

3.3.1 Layer mapping

The complex modulation symbols to be transmitted are mapped onto one or several layers in layer mapping. The complex-valued modulation symbols \mathbf{x} for power domain multiplexed signal shall be mapped onto the layer $\mathbf{x}(j) = [\mathbf{x}^{(0)}(j) \dots \mathbf{x}^{(\nu-1)}(j)]^T, j = 1, \dots, M_{symbol}^{layer}$ where ν is the number of layers and M_{symbol}^{layer} is the number of modulation symbols per layer.

For spatial multiplexing, the layer mapping shall be done according to Table 6.3.3.2-1 in 3gpp release 14 [30]. The number of layers ν is less than or equal to the number of antenna ports P used for transmission of the physical channel. Here $\nu=2$ for two transmitted antennas. In this case two users' information bits are separately modulated and combined to a one sequenced with the predefined power ratio. Then the concatenated signal will be layer mapped to transmit using two antennas. Therefore according to [30], layer mapped signal is defined as $\mathbf{x}^{(0)}(j) = \mathbf{x}(2j)$ and $\mathbf{x}^{(1)}(j) = \mathbf{x}(2j + 1)$ where $M_{symbol}^{layers} = M_{symbol}^0/2$ for single modulated sequence is mapped to the two layers.

3.3.2 Pre-coding for Large Delay Cyclic Delay Diversity

Large Delay Cyclic Delay Diversity (CCD) is a kind of transmit diversity mechanisms implemented by applying a different phase delay. The idea is to send on each antenna a circularly shifted version of the same OFDM symbol in the time domain. Hence, the temporal delay introduced on each antenna is transformed into a cyclic delay in the CDD scheme as shown in Fig. 3.5.

The precoder takes a block of vectors $\mathbf{x}(j) = [\mathbf{x}^{(0)}(j) \dots \mathbf{x}^{(\nu-1)}(j)]^T, j = 0, 1, 2, \dots, M_{symbol}^{layer}$ as the input from the layer mapping and generates a block of vectors $\mathbf{x}_{CDD}(j) = [\dots x_{CDD}^{(p)}(j) \dots]^T, j = 0, 1, 2, \dots, M_{symbol}^{ap} - 1$ to be mapped onto resources on each of the antenna ports, where $x_{CDD}^{(p)}(j)$ represents the signal for antenna port p .

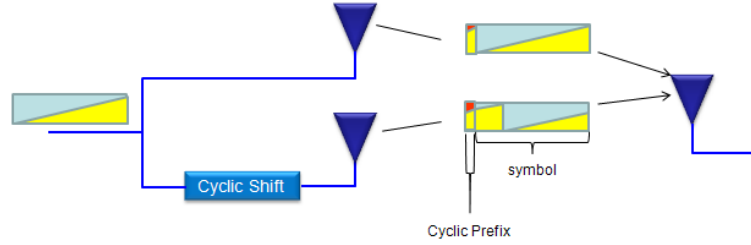


Figure 3.5: Cyclic Delay Diversity

[31]

Precoding and CDD is defined for different Transmission Modes in LTE in 3gpp release [30] according to Table 3.3.

In this research we propose the receiver for TM3 because we used open loop MIMO system. Precoding for TM3 is defined in [30] as per (3.3).

$$\begin{bmatrix} \mathbf{x}_{CDD}^{(0)}(j) \\ \mathbf{x}_{CDD}^{(1)}(j) \end{bmatrix} = W(i)D(i)U \begin{bmatrix} \mathbf{x}^{(0)}(j) \\ \mathbf{x}^{(1)}(j) \end{bmatrix}, \quad (3.3)$$

$$\text{where } W(i) = 1/\sqrt{2} \begin{bmatrix} 1 & 0 \\ 0 & 1 \end{bmatrix}, D(i) = \begin{bmatrix} 1 & 0 \\ 0 & e^{-j2\pi i/2} \end{bmatrix} \text{ and } U = 1/\sqrt{2} \begin{bmatrix} 1 & 1 \\ 1 & e^{-j2\pi/2} \end{bmatrix}.$$

TM	DL Transmission Scheme	No of Antenna Ports	CDD Type
TM1	Single Antenna Port (SISO or SIMO)	1	No CDD
TM2	Transmit Diversity	2	No CDD
TM3	Open-Loop Spatial Multiplexing	2	Large CDD
TM4	Closed-Loop Spatial Multiplexing	2	No CDD
TM5	Multi-User MIMO	2	No CDD
TM6	Closed loop Rank 1 Spatial Multiplexing	1	No CDD
TM7	Single Antenna Port Beam Forming	1	No CDD
TM8	Dual Layer Beam Forming	2	No CDD

Table 3.3: Transmission modes define in LTE

[32]

3.3.3 OFDMA mapping

The transmitted signals are converted to N number of parallel streams after layer mapping, which is the number of subcarriers. The number of subcarriers in LTE is defined according to the available transmission BW as mentioned in Table 3.4.

Channel BW	5 MHz	10MHz	20MHz
FFT length(N)	512	1024	2048
Subcarriers per symbol	300	600	1200

Table 3.4: FFT length in LTE

[30]

After the IFFT operation, cyclic prefixes are added according to Table 6.2.3-1 in [30] and parallel streams are converted back to a single stream for transmission. There are two types of cyclic prefix used in LTE such as normal cyclic prefix and extended cyclic prefix. Normal cyclic prefix is used in urban cells and high data rate applications while the extended cyclic prefix is used in special cases like multi-cell broadcast and in very large cells because the extended cyclic prefix reduce the data rate while minimizing the ISI effect [31].

Chapter 4

PROPOSED RECEIVER SCHEMES

4.1 Introduction

As stated before, there are performance issues in MMSE based detectors and complexity can not be handled in ML based detectors . In order to achieve improved trade off between complexity and performance we propose a K-Best sphere detector based detector for successive interference cancellation and the signal detection of the cell-center user. In the K-Best sphere detector, the cardinality of signal constellation decides the number of branches in the search tree as explained in section 2.2.3. We consider the joint constellation which is generated by superimposing cell-center user and cell-edge user signal constellations, for the cell-edge user signal detection at the cell-center user. Joint constellation is briefly discussed in Section 3.2.1.

4.2 Proposed Receiver Structure for NOMA in Single-Carrier MIMO Systems

The proposed downlink NOMA receiver for the cell-center user with QPSK modulation is shown in Fig 4.1 for a single carrier MIMO systems. Since the cell-edge user signal is stronger at the cell-center user, first the cell-edge user signal is detected and the interference from the cell-edge user is calculated to remove from the received signal of cell-center user. Then the cell-center user signal is detected and demodulated to get the estimated transmitted signal vector of cell-center user. Signal detection in details with mathematical formulation is present in this section.

$$\mathbf{y}_i = \mathbf{H}_i \mathbf{x} + \mathbf{n}_i. \quad (4.1)$$

\mathbf{y}_i represents the received signal vector at user i , where \mathbf{H} is a 2×2 Rayleigh channel matrix, assumed to be perfectly known at the receiver with independent elements h_{ij} of zero mean and

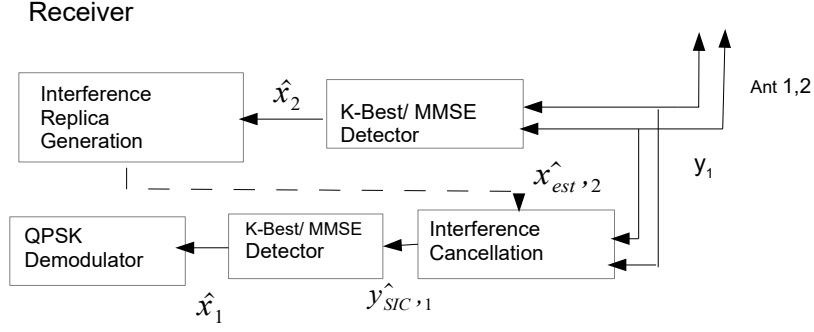


Figure 4.1: Proposed receiver for cell-center user

unit variance complex Gaussian distribution. \mathbf{H}_i represents the 2×2 channel matrix for the user i . We assume that the channel is quasi static, i.e., the channel coefficients are vary from block to block independently. \mathbf{n}_i is an independent and identically distributed (i.i.d) AWGN vector of user i , where $E[\mathbf{n}_i \mathbf{n}_i^H] = \sigma^2 \mathbf{I}$ and \mathbf{I} is a 2×2 identity matrix and σ^2 is the noise variance. \mathbf{H}_i is defined in (4.2) according to [6]:

$$\mathbf{H}_i = \sqrt{p_i} \mathbf{H}. \quad (4.2)$$

y_1 is the received signal of the cell-center user and it is fed to the MMSE or K-Best detector to detect the cell-edge user signal. Here we are not using channel coding. Therefore \hat{x}_2 , the estimated symbols of cell-edge user is directly used to generate the interference replica $\hat{x}_{rep,2}$ according to (4.3).

$$\hat{x}_{rep,2} = \mathbf{H}_1 \sqrt{p_2} \hat{x}_2. \quad (4.3)$$

$$\hat{y}_{sic,1} = y_1 - \mathbf{H}_1 \sqrt{p_2} \hat{x}_2. \quad (4.4)$$

$\hat{y}_{sic,1}$ is the cell-center user (user 1) received signal after cancelling the interference of the cell-edge user (user 2). It is then fed to the MMSE or K-Best detector to detect the transmitted symbols of the cell-center user. The output from the detector is fed into the symbol demapper and the cell-center user signal \hat{u}_1 is detected. \hat{x}_2 and \hat{x}_1 change with the usage of MMSE detector and K-Best detector and resent in the subsections 4.2.1 and 4.2.2.

In this research we considered the performance of four receiver schemes, by changing the type of receiver, used for detection of the cell-center user and the cell-edge user for SIC as mentioned in Table 4.1. To the best of our knowledge, already existing receivers are not considered K-best detector based detector for SIC in NOMA systems. The error performance of Receiver Scheme-1 with channel coding and OFDMA modulation is discussed in [6] and our contribution is to discuss the improvement of BER performance using K-Best detector.

Receiver Scheme	user2 (Cell Edge User)	user1 (Cell Center User)
Receiver Scheme-1 (RS-1)	MMSE	MMSE
Receiver Scheme-2 (RS-2)	MMSE	K-Best
Receiver Scheme-3 (RS-3)	K-Best	MMSE
Receiver Scheme-4 (RS-4)	K-Best	K-Best

Table 4.1: Receiver Schemes Tested in the research

4.2.1 MMSE Detector for Power Domain NOMA

The MMSE receiver is a linear receiver with low complexity as discussed in detail in Section 2.2 and the MMSE filtering matrix can be generated based on (2.3). With NOMA, the signals of both users are present at the cell-center user and the filtering matrix is changed as follows :

$$\mathbf{G}_{MMSE} = (\mathbf{H}_2\mathbf{H}_2^H + \mathbf{H}_1\mathbf{H}_1^H + \sigma^2\mathbf{I}_{n_r})^{-1} \mathbf{H}_2^H \quad (4.5)$$

4.2.2 K-Best Detector for Power Domain NOMA

As stated earlier, the signals of both users are present at the cell-center with NOMA, hence we used the joint constellation discussed in 3.2.1 for cell-edge user detection. Even though the cell-center user also can be directly detected using joint constellation, we detect the cell-edge user first and SIC is then performed to detect the cell-center user because the PED between the joint constellation vary with power allocation ratios p_1 and p_2 . When $p_1 : p_2$ ratio is increasing, constellation points are getting closer and difficult to detect separately as illustrated in Fig 3.3.

Initially in this study, we tried to detect the cell-edge user signal at the cell-center, without considering the joint constellation. That means considering the cell-center user signal as interference. However the performance was worse than MMSE-SIC receiver as shown in Fig

4.2. In power domain NOMA, signal constellation is changed for transmitted signal and it is required to check the ED with the new constellation for correct detection of signals.

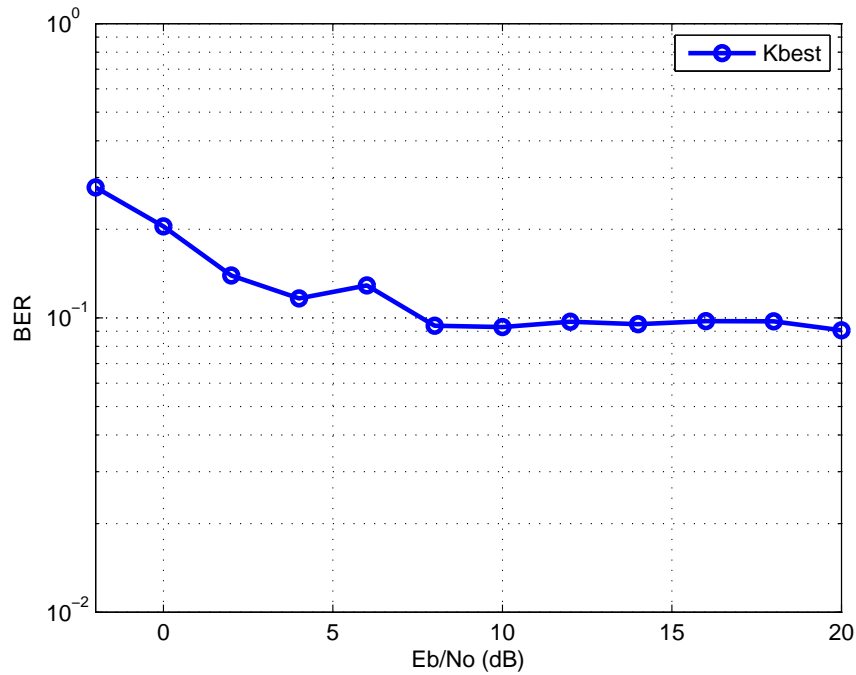


Figure 4.2: BER performance without considering joint modulation

Even though the number of branches in search tree is exponentially increased with the constellation, the complexity can be reduced without significant performance degradation by carefully selecting the K value. As an example, when the two users are using QPSK modulation, number of elements in joint constellation is 16. Therefore there are 16 branches at the root layer of the search tree and each parent node is having 16 child nodes. However according to the simulations, we can select the K value which is less than 16, without significant performance degradation.

4.3 Receiver for NOMA in MIMO-OFDMA Systems

In the previous section we present the receiver for NOMA in single carrier MIMO systems. However according to the 3Gpp Release 14, LTE air interface is based on OFDMA. In this section, we present a receiver for NOMA in MIMO- OFDMA Systems. Fig. 4.3 shows the proposed receiver block diagram for OFDMA systems. the SIC detection is similar and

OFDMA demapping and CDD removal is introduced for OFDMA systems.

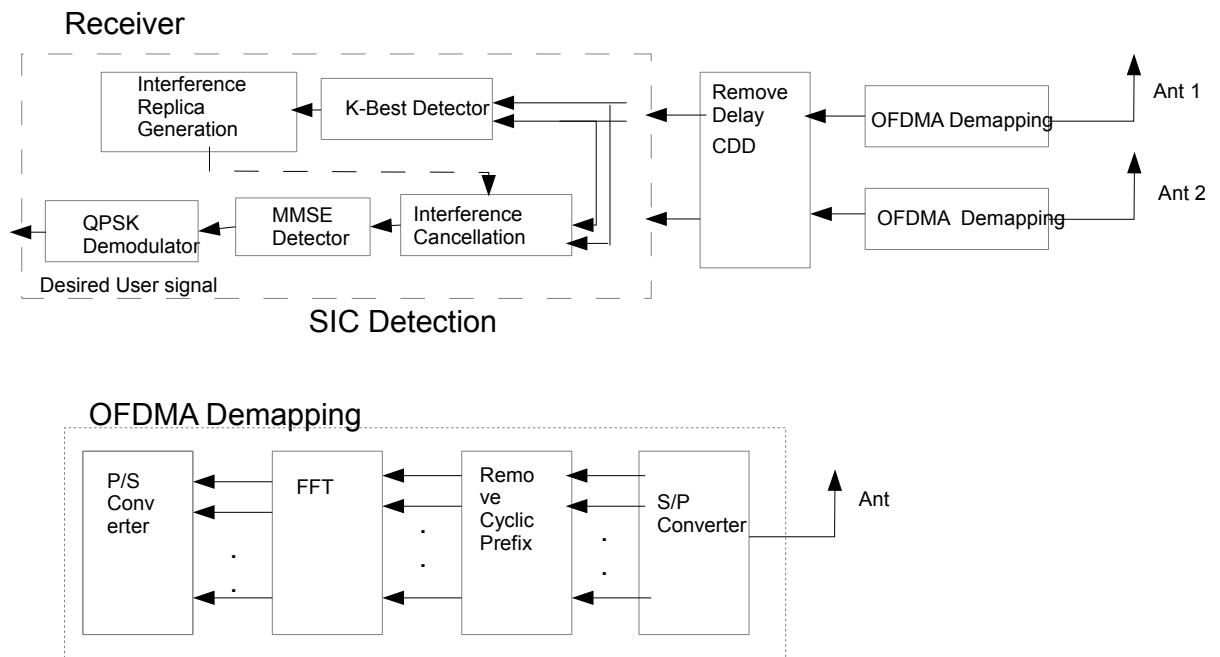


Figure 4.3: Receiver for NOMA in MIMO-OFDMA systems

Chapter 5

SIMULATION RESULTS AND DISCUSSION

5.1 Preliminary Results

We carried out MATLAB simulations to evaluate the BER performance of different MIMO detectors during the literature survey. Some of the simulation results comparing the performance of K-Best detector with MMSE detector and ML detector are presented in this section. The simulations are carried out for Rayleigh channel matrix, assumed to be perfectly known at the receiver with independent elements of zero mean and unit variance complex Gaussian distribution. We assume that the channel is quasi static with the block length of 2048. Simulation results were obtained for different modulation schemes and MIMO schemes for single user, single carrier MIMO systems.

Fig 5.1 shows the BER for single user 2x2 MIMO system for the ML detector, the MMSE detector and the K-Best detector. It is clear from these results, that the K-Best sphere detector approaches the almost similar performance to the ML detector when the K value is closer to the cardinality of constellation and the performance is degraded closer to MMSE detector when the $K=1$, i.e., very small K value. The difference in BER performance in between the MMSE detector and the K-best detector can be clearly identified in higher E_b/N_0 values.

The simulation results for 4x4 MIMO systems with BPSK modulation is shown in Fig 5.2. Similar to the results for 2x2 MIMO systems in Fig 5.1, K-Best detector with reasonable K value shows a considerable improvement over MMSE detector for 4x4 MIMO systems as well. Further it is clear that we can reduce the K value up to some level without a significant performance degradation. The almost similar observations can be made on Fig. 5.3 for 4x4 MIMO with QPSK modulation.

It is observed that improved trade off between the error performance and complexity can be achieved using the K-best detector. However if the K value is arbitrary decreased, per-

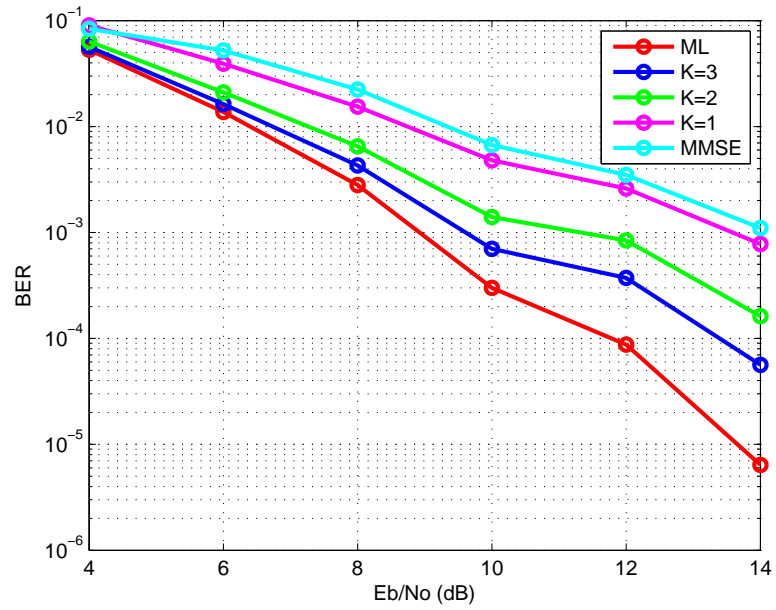


Figure 5.1: BER performance for 2x2 MIMO with QPSK

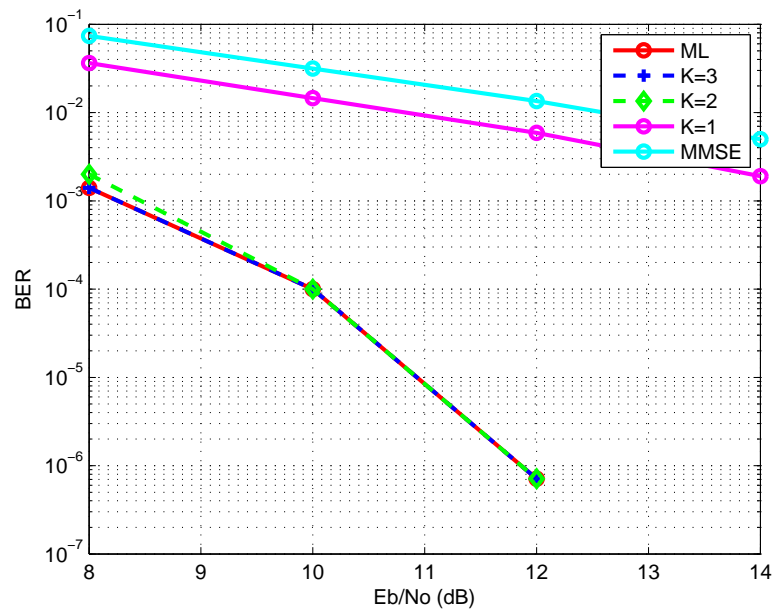


Figure 5.2: BER performance for 4x4 MIMO with BPSK

formance of K-Best detector is degraded near to that a MMSE detector. Therefore the K values should be properly selected based on the required accuracy and the affordable complexity.

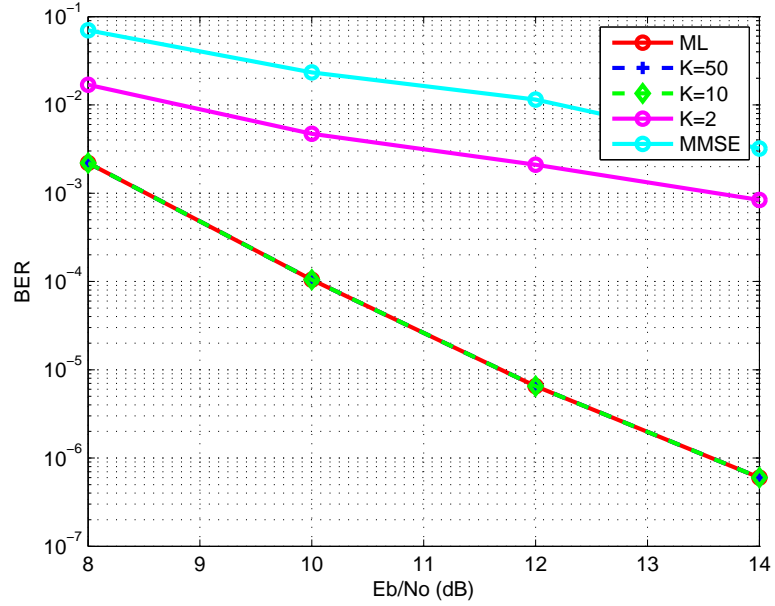


Figure 5.3: BER performance for 4x4 MIMO with QPSK

5.2 Assumptions and System Parameters

We carry out link-level simulation to assess the impact of proposed receiver schemes presented in Table 4.1 with different power allocation ratios in between cell-center user and cell-edge user (User 1: User 2). The BER performance of NOMA in the downlink of a SU-MIMO-OFDMA system is investigated. At the BS transmitter, the binary information sequence is modulated using QPSK or 16-QAM. As stated earlier channel coding is not considered in simulations. The symbol sequences of both the UEs are non-orthogonally multiplexed in the power domain based on a predefined power ratio, $p_1 : p_2$. The combined signal is transmitted over the Rayleigh fading channel. At the cell-center user, symbol level SIC is applied to detect the cell-center user signal. We compare the BER performance of the cell-center user with different system parameters such as using MMSE receiver and K-Best receiver, different power allocation ratios, K values for K-Best detector, modulation schemes and MIMO levels.

The system parameters are summarized in Table 5.1

Parameter	Value
System BW	20MHz
FFT length	2048
Subcarriers per symbol	1200
Subcarrier separation	15kHz
Subframe length	1 ms
Symbol duration	Effective data: $66.67\mu s$ + CP: $4.69\mu s$ (normal CP)
Channel Coding	not used
Antenna configuration	2x2 and 4x4
Receiver	MMSE based SIC , K-Best based SIC
Channel Model	Rayleigh fading channel

Table 5.1: System parameters used in simulation

5.3 Results obtained for NOMA in Single-Carrier MIMO Systems

In Fig 5.4, the BER performance obtained using different receiver schemes are shown for a 2x2 MIMO systems with QPSK. The power allocation ratio used is $p_1 : p_2 = 0.3 : 0.7$ and QPSK modulation is used for both the users. The size of joint constellation is 16. Here we consider $K=14$ for the cell-edge user signal detection at the cell-center user and $K=3$ for the cell-center user signal detection after interference cancellation. It is clear that the receiver scheme 1 and 2 (RS-1 and RS-2) are having an almost similar results while the receiver scheme 4 (RS-4) is the best. In RS-1 and RS-2, MMSE detector is used for cell-edge user detection at the cell-center user. Since the error performance of the MMSE receiver is poor with interference, the cell-edge user detection is more erroneous. Therefore due to the less accurate detection of the cell-edge user signal, it is not possible to get a considerable improvement by using K-best sphere detector for the cell-center user detection in RS-2 .

In RS-3 and RS-4, the K-best sphere detector is used to detect the cell-edge user signal. It can be observed from Fig 5.4, nearly 2 dB and 4 dB gains are observed at BER of 10^{-3} for RS-3 and RS-4 respectively, compared to RS-1. However using K-Best detector for both the users is increased the complexity and the time taken to the signal detection . According to [7], the performance of ideal SIC represents an upper bound for DL NOMA receivers which is the scenario with perfect interference cancellation. In 5.4, the ideal K-Best and the ideal ML are present the error performance for transmitting only the cell-center user signal, it shows the

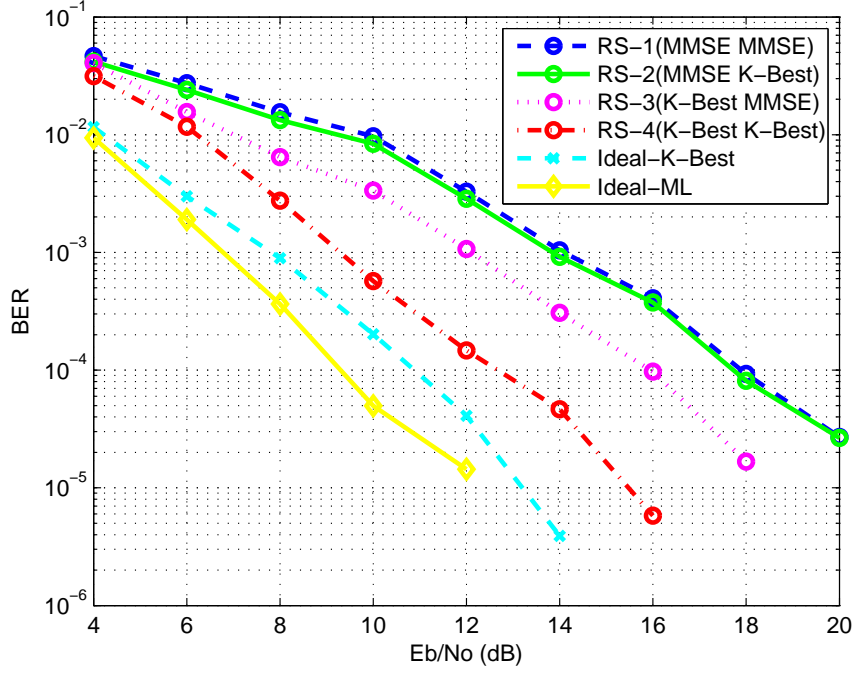


Figure 5.4: BER performance for 2x2 MIMO NOMA system

scenario where interference is perfectly removed for cell-center user detection. Even though the ML detector is the optimal detector, implementation in practical receivers may not be feasible due to complexity. Therefore, we take the performance of Ideal K-Best detector as the reference performance since the complexity can be managed. Compared with the reference, RS-1 and RS-2 are deviated widely from the ideal situation and RS-4 is the closest performance.

It can be observed from Fig 5.5, the BER performance for different power levels for RS-1 and RS-3. That is the detector is changed only for the cell-edge user signal detection for SIC and the same MMSE detector is used to detect the cell-center user after interference cancellation in RS-1 and RS-3. In the Fig 5.5, different colours in lines with a marker indicate different $p_1 : p_2$ ratios, i.e., $p_1 : p_2 = 0.2 : 0.8, 0.3 : 0.7$ and $0.4 : 0.6$ where $p_2 = 1 - p_1$ and line patterns indicate the two receiver schemes. The K value for the K-Best detector is kept at 14 for RS-3. It is clear that when p_1 is increased, the error performance degrades in both the receiver schemes. This is due to the fact that, when p_1 increase, p_2 decreases and therefore, the cell-edge user signal detection at the cell-center user is more erroneous. This is because of the effect of interference caused by the cell-center user to the cell-edge user detection is increased.

When $p_1 = 0.4$, RS-3 offers 4 dB gain at BER of 10^{-3} over RS-1, while the gain is only

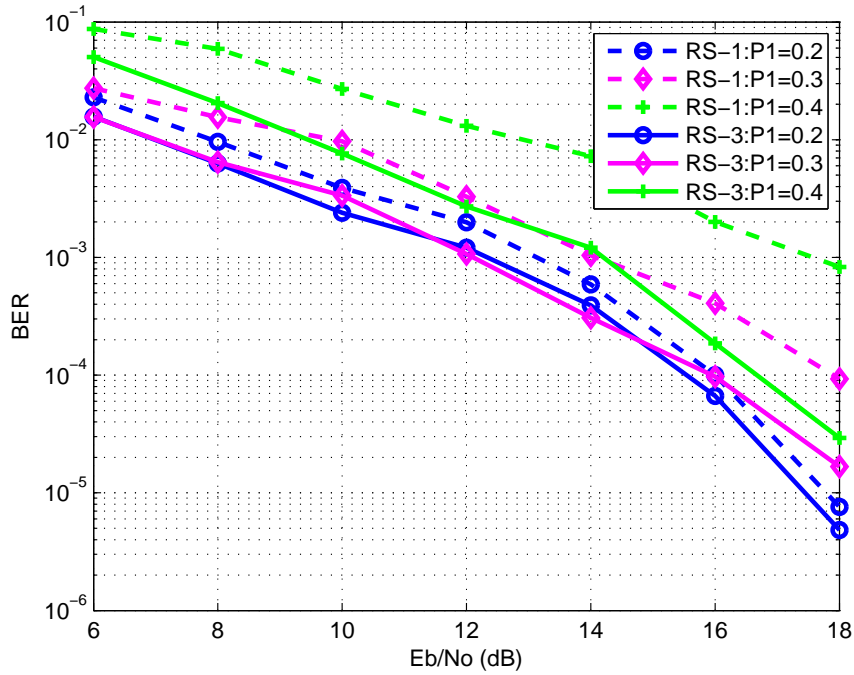


Figure 5.5: BER performance for different power levels with RS-1 and RS-3

2 dB for $p_1 = 0.3$. Therefore, using the K-best based receiver is more useful in instances where the cell-center user and cell-edge user power levels are comparable. As mentioned in Section 1.1.1, the power allocation ratio has an upper bound with MMSE based SIC receivers. However according to the observation in Fig 5.5, the K-best receiver offers considerable gain in error performance with higher $p_1 : p_2$ ratios compared to MMSE receivers.

The BER performance for different power levels at $E_b/N_0 = 16dB$ is shown in Fig. 5.6 for RS-1 and RS-3. The increased BER can be observed for both the receiver schemes when the p_1 increases because then the p_2 decreases and interference increases. It is clearly observed that the RS-3 is having better performance with the increase p_1 ratios compared to RS-1.

Fig 5.7 compares the BER performance of receiver schemes obtained using different K values in the K-best detector used to detect the cell-edge user for SIC. Here we used the power ratios of $p_1 : p_2 = 0.3 : 0.7$ and QPSK as the modulation for both the users. Then the joint constellation of the transmitted signal has 16 symbols. Therefore we use $K=14, 10, 7$ for K-best receiver to detect cell-edge user and the performance is compared with RS-1 and RS-4. $K=3$ is used for cell-center user decoding for RS-4. It can be observed from Fig ??, RS-3 offers better performance than RS-1 for all the K values used in the simulations. Therefore, it's possible to

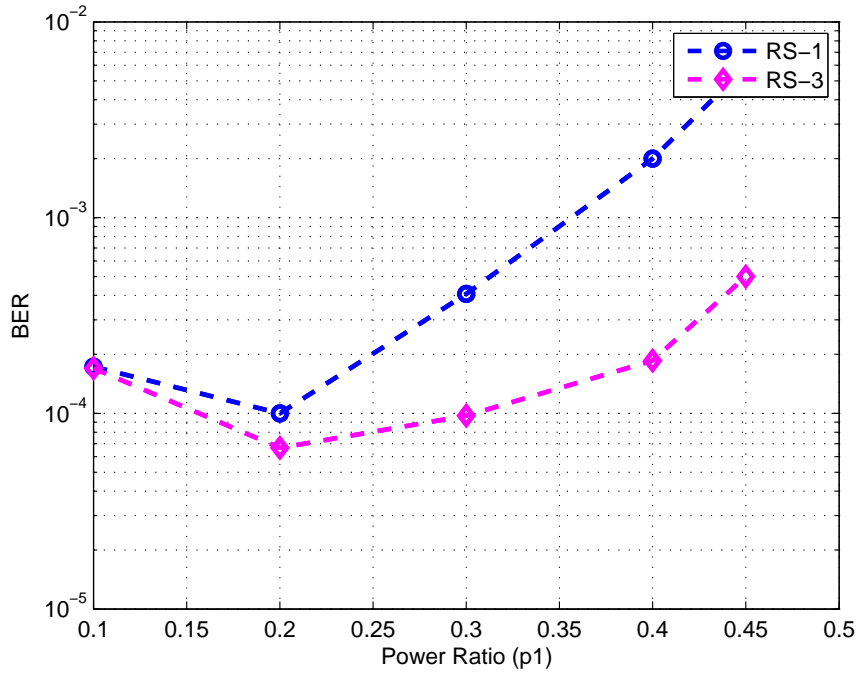


Figure 5.6: BER variation with power ratio at $E_b/N_0=16$ dB

reduce the K value without a significant performance degradation. This is because in the K -best algorithm, it selects the K number of best paths to extend the search tree. Even though the K value is reduced, only the worst paths are removed from the search list and the search algorithm continues with the paths related to the most probable symbol. Therefore the complexity and the time taken to detect the symbols can be considerably reduced without significant performance loss by reducing the K value used for K -best receiver.

Generally, modulation level is selected considering the channel condition of the user. If the user has a better channel condition, a higher modulation level is assigned to provide a higher data rate. In Fig 5.8, we compare the performance observed with 16-QAM modulation for the cell-center user and QPSK modulation for the cell-edge user, along with power allocation ratio equals to $p_1 : p_2 = 0.3 : 0.7$ in 2×2 MIMO system for RS-1 and RS-3. In this case, joint constellation has 64 symbols and we used $K=50$ for cell-edge user signal detection in RS-3 and RS-4. Further, we changed the K values such as $K=15,10$ in the K -best receiver to compare the BER performance. However it was observed that the performance is almost similar for different K values. Therefore it is confirmed that reducing the K value is not severely affected to the performance.

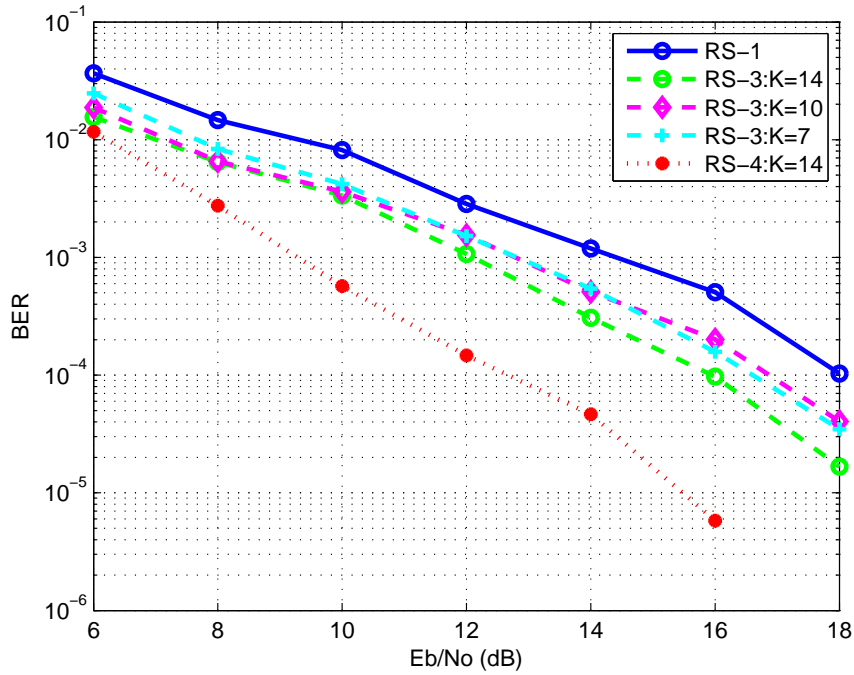


Figure 5.7: BER performance for different K values

Fig 5.9 compares the performance of 4x4 MIMO systems with power domain NOMA with power allocation ratio of $p_1 : p_2 = 0.3 : 0.7$ and QPSK modulation. Considering the transmitted signal, joint constellation has 16 symbols and we use K=14 and K=3 for the K-best detectors used for cell-edge user and cell-center user detection respectively. In 4x4 MIMO systems, search tree has 5 layers including the root layer. However, only a K number of selected paths are extended to the lower layers in the search algorithm. Similarly to Fig.5.4, RS-1 and RS-2 are having almost similar error performance. Nevertheless RS-2 outperforms RS-1 due to the K-Best detector used in the cell-center user detection. RS-3 and RS-4 offers a few dB gain compared to RS-1 and the gain improves compared to 2x2 MIMO.

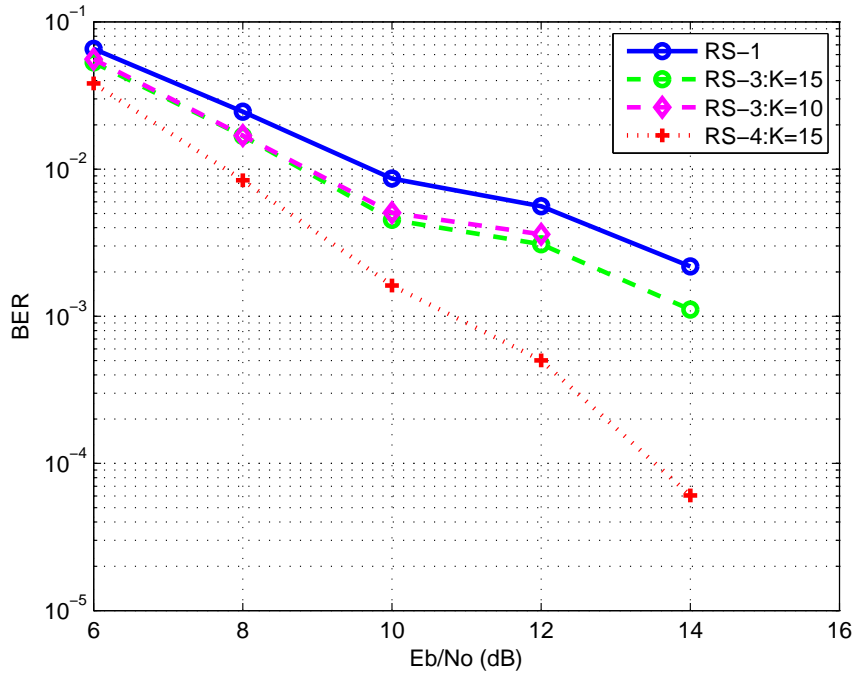


Figure 5.8: BER performance by using QPSK for cell-edge user and 16-QAM for cell-center user

5.4 Results obtained for NOMA in MIMO-OFDMA Systems

We discuss the BER performance obtained for NOMA in MIMO-OFDMA system in this section. In the previous section we compared the performance of all the four receiver schemes and concluded that RS-1 and RS-2 have almost similar performance and RS-4 has the best performance with highest computational complexity. Therefore we concluded that the best receiver scheme is RS-3 compromising the performance with complexity. Therefore in this section we compare the BER performance of RS-3 with respect to RS-1 and ideal scenario.

The BER performance obtained for NOMA in MIMO-OFDMA systems using receiver schemes RS-1 and RS-2 are shown in Fig. 5.10 . The ideal scenario is the BER of the cell-center user signals detection considering no interfering user, i.e., the cell-edge user. We use $p_1 : p_2 = 0.3 : 0.7$ power allocation and $K = 14$ for K-Best detector used to detect the cell-edge user for SIC. Similar to the single carrier system, RS-3 has nearly 3 dB gain at BER of 10^{-3} compared to RS-1. However we can observe a considerable performance gap to the ideal K-Best detector. Mainly this gap can be reduced with channel coding.

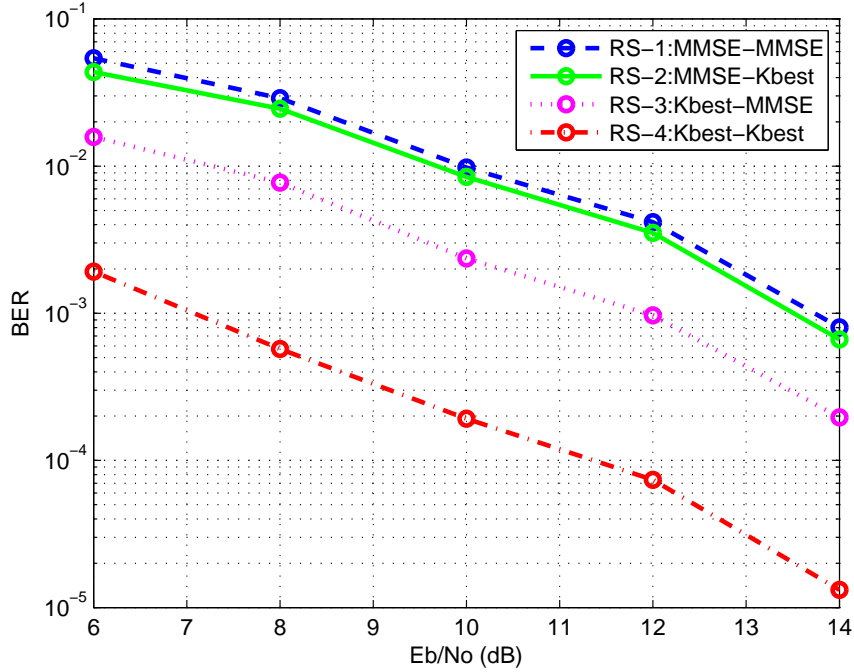


Figure 5.9: BER performance for 4x4 MIMO

The BER performance with different power allocation ratios in between two users are discussed in Fig. 5.11. If the power ratio of the cell-center user (p_1) increases, interference also increases as explained in the previous section. As a result, the BER also increases for both the receiver schemes with increasing p_1 . We compare the performance for RS-1 and RS-3 with three power allocation ratios such as $p_1 : p_2 = 0.2 : 0.8$, $p_1 : p_2 = 0.3 : 0.7$ and $p_1 : p_2 = 0.4 : 0.6$. Considering a situation where p_1 is very smaller compared to p_2 , RS-3 does not have much improvement compared to RS-1 but when $p_1 : p_2$ ratios are comparable, RS-3 is having nearly 4 dB improvement compared to RS-1.

Therefore it is clear that the proposed receiver is more important in the situations where the interference level is high. Further in practical situations there are more than two users multiplexed in NOMA systems. Then the users may have nearly the same power levels. In that situation MMSE based SIC receivers may not be feasible while the proposed receiver may have acceptable performance with increased complexity.

The performance of K-Best detector with different K values are presented in Fig. 5.12. Power allocation ratios are kept at $p_1 : p_2 = 0.3 : 0.7$ for this simulation and K value used for the K-best detector are changed. Similar to the single carrier systems, reducing K value is not

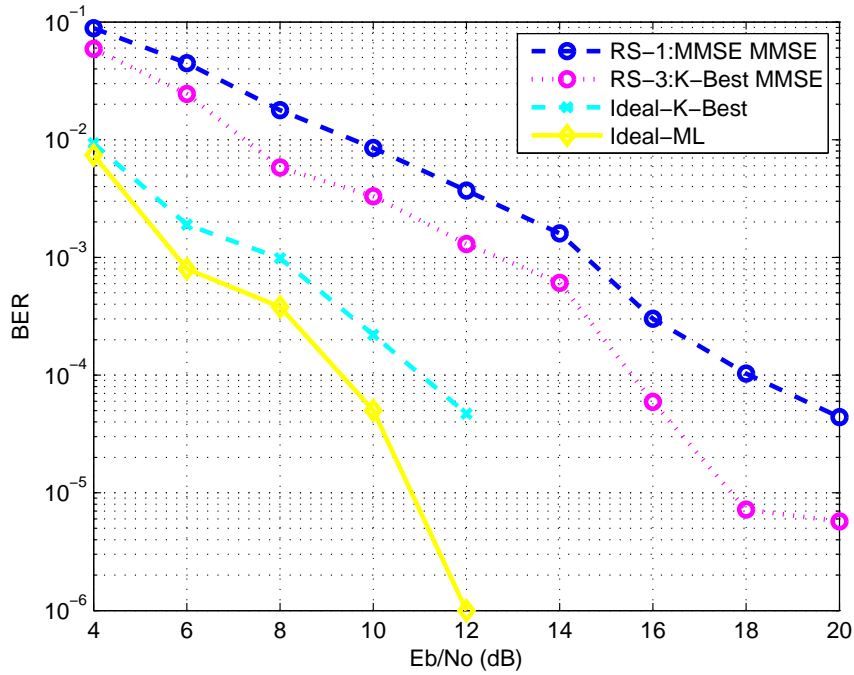


Figure 5.10: BER performance for OFDMA system

severely affected to the BER performance. Even with the small K values RS-3 performs better than RS-1. However reducing K value will directly reduce the complexity and the time taken for detection of the K-Best receiver.

As discussed in this section, proposed receiver is feasible with MIMO-OFDMA systems and having significantly better performance compared to MMSE based SIC receivers. According to [6], MMSE based symbol level SIC receiver is having very poor performance even with channel coding and they have proposed MMSE based code word level SIC receiver for NOMA. However we consider the symbol level SIC receiver since we didn't use the channel coding and still we obtained good BER performance for NOMA with the proposed receiver.

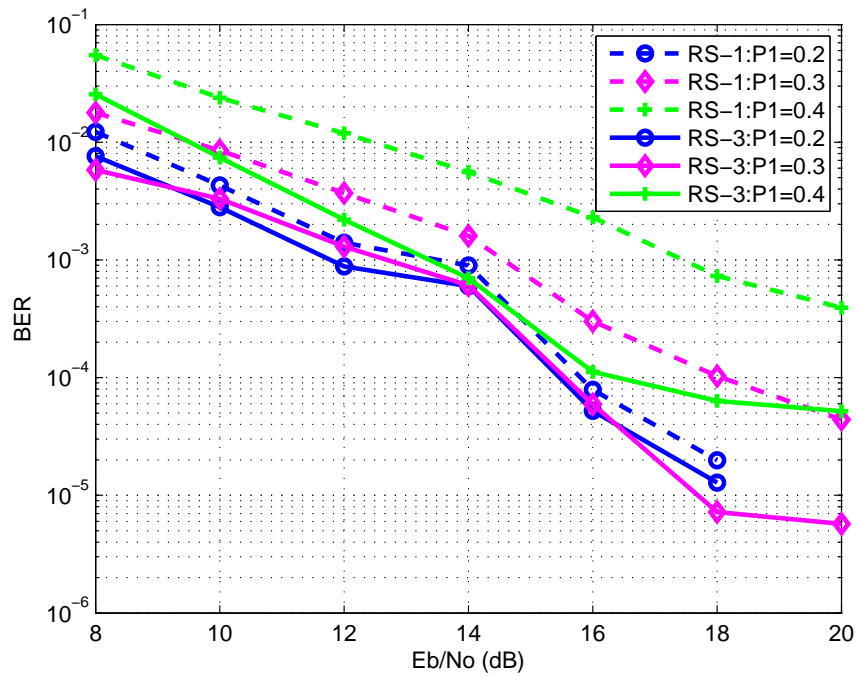


Figure 5.11: BER performance for OFDMA with different power levels

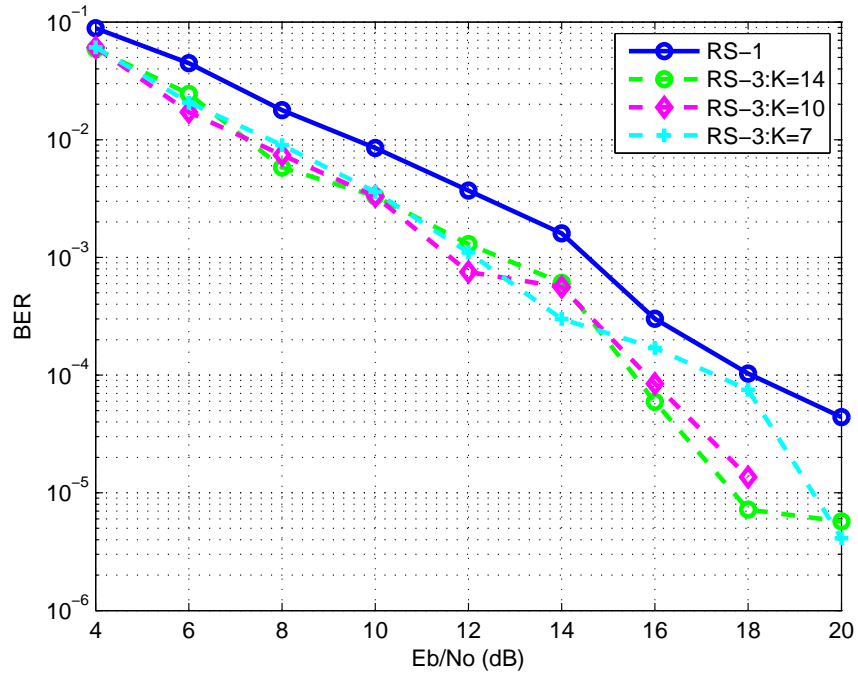


Figure 5.12: BER performance for OFDMA with different K values

Chapter 6

CONCLUSION AND FURTHER RESEARCH

6.1 Conclusion

The main objective of this research study was to develop an efficient receiver for the down-link of MIMO-NOMA- OFDMA system to obtain improve trade off between performance and complexity over conventional receivers. We proposed a K-best Sphere Detector based receiver for power domain NOMA in the SU-MIMO systems. We compared the BER performance of the proposed receiver with the MMSE-based SIC receiver and the ideal SIC receiver, in which we assumed that there was no any residual interference of the cell edge user after SIC.

The simulation results have demonstrated that in order to obtain improved performance, it is required to use a K-best detector for the cell-edge user detection at the cell-center user, i.e., for the interference cancellation stage. This is due to the fact that if the MMSE based receiver is used for cell-edge user detection, the poor performance of MMSE based receiver affects to the cell-center user detection due to the residual errors. Though a K-best detector can also be used for detection of the symbols of the cell-center user, the performance improvement obtained over using a K-best detector only for detecting the cell-edge user is significant. Furthermore using the K-best detector for both the cell-center user and the cell-edge user detection is increased the computational complexity and the time taken to detect the symbols. Based on the simulation results it can be concluded that using the K-Best detector only at the cell-center user to detect the cell-edge user is the best scenario which compromises between performance and complexity.

It was observed from the simulation results that the performance of the proposed receiver is better than the MMSE based receiver even after using small K values for the K-best detector which significantly reduce the computational complexity. This is due to the fact that always K number of paths with minimum PED will be retain in the search list. The proposed receiver is

having much better performance than MMSE based SIC receiver even with the two users are having comparable power levels. That concluded the proposed receiver is more suitable when the interference level is high.

However there are certain limitations in the proposed receiver. The complexity is exponentially increased with the increased number of users. Since we consider the joint modulation to detect the cell-center user signal, size of joint constellation is exponentially increased with number of users and hence the number of branches at a given parent node of the search tree also increased similar to the size of the constellation. However the complexity can be managed by selection an appropriate K value. Therefore the proposed receiver is not recommended for large number of users.

Here in power domain NOMA, the transmitted signal power is decided according to the channel condition. Therefore the proposed receiver can not be used with the users having similar channel conditions. As an example, with the users at a similar distance from the telecommunication tower. Therefore power domain NOMA and the proposed receiver is more suitable to combine with OFDMA where it enables different users with different channel conditions to share the same RB.

6.2 Suggestions for Further Research

A few suggestions for further research areas are summarized in this section.

1. In this research, we have only focused on uncoded systems and have presented the simulation results without channel coding. More improvements to the BER can be achieved using channel coding and can be checked the gap between ideal SIC performance to the proposed receiver with channel coding.
2. We have considered hard decision K-Best detector for this research study. Further improvement can be tested with iterative based soft output K-best detector which is already tested for MIMO-OFDMA systems. In the case of coded MIMO system, the performance can be improved by iteratively exchanging soft information between the MIMO detector and the channel decoder.
3. Here we consider a two user detection scenario (cell-center user and cell-edge user) for power domain NOMA. performance of the proposed receiver can be evaluated for more users with different power allocation ratios among them. The upper bound for

number of users who can share the same time, frequency resources in power domain can be confirmed and different power allocation methods also an emerging topic to discuss

4. Furthermore, future work could be focus on using K-Best detector to directly detect the cell center user without SIC. This will reduce the complexity and the detection time. Since the joint constellation is changing with the power allocation ratio, performance of direct detection should be tested with different power levels.

Bibliography

- [1] L. Dai, B. Wang, Z. Ding, Z. Wang, S. Chen, and L. Hanzo. A Survey of Non-Orthogonal Multiple Access for 5G. *IEEE Communications Surveys Tutorials*, 20(3):2294–2323, Third quarter 2018.
- [2] Ericsson. Ericsson Mobility Report. <https://www.ericsson.com/res/docs/2016/ericsson-mobility-report-2016.pdf>, 2016. Accessed: 2019-06-15.
- [3] Mahmoud Aldababsa, Mesut Toka, Selahattin Gokceli, Gunes Karabulut Kurt, and Oguz Kucur. A Tutorial on Nonorthogonal Multiple Access for 5G and Beyond. *arXiv e-prints*, page arXiv:1902.08992, Feb 2019.
- [4] A. Li, Y. Lan, X. Chen, and H. Jiang. Non-orthogonal Multiple Access (NOMA) for future downlink radio access of 5G. *China Communications*, 12(Supplement):28–37, December 2015.
- [5] Z. Ding, X. Lei, G. K. Karagiannidis, R. Schober, J. Yuan, and V. K. Bhargava. A Survey on Non-Orthogonal Multiple Access for 5G Networks: Research Challenges and Future Trends. *IEEE Journal on Selected Areas in Communications*, 35(10):2181–2195, Oct 2017.
- [6] K. Saito, A. Benjebbour, Y. Kishiyama, Y. Okumura, and T. Nakamura. Performance and design of SIC receiver for downlink NOMA with open-loop SU-MIMO. In *2015 IEEE International Conference on Communication Workshop (ICCW)*, pages 1161–1165, June 2015.
- [7] C. Yan, A. Harada, A. Benjebbour, Y. Lan, A. Li, and H. Jiang. Receiver Design for Downlink Non-Orthogonal Multiple Access (NOMA). In *2015 IEEE 81st Vehicular Technology Conference (VTC Spring)*, pages 1–6, May 2015.

- [8] Y. Cai, Z. Qin, F. Cui, G. Y. Li, and J. A. McCann. Modulation and Multiple Access for 5G Networks. *IEEE Communications Surveys Tutorials*, 20(1):629–646, First quarter 2018.
- [9] A. Benjebbour, Y. Saito, Y. Kishiyama, A. Li, A. Harada, and T. Nakamura. Concept and practical considerations of non-orthogonal multiple access (NOMA) for future radio access. In *2013 International Symposium on Intelligent Signal Processing and Communication Systems*, pages 770–774, Oct 2013.
- [10] Z. Ding, F. Adachi, and H. V. Poor. The Application of MIMO to Non-Orthogonal Multiple Access. *IEEE Transactions on Wireless Communications*, 15(1):537–552, Jan 2016.
- [11] M. M. El-Sayed, A. S. Ibrahim, and M. M. Khairy. Power allocation strategies for Non-Orthogonal Multiple Access. In *2016 International Conference on Selected Topics in Mobile Wireless Networking (MoWNeT)*, pages 1–6, April 2016.
- [12] J. Zhu, J. Wang, Y. Huang, S. He, X. You, and L. Yang. On Optimal Power Allocation for Downlink Non-Orthogonal Multiple Access Systems. *IEEE Journal on Selected Areas in Communications*, 35(12):2744–2757, Dec 2017.
- [13] R. Hoshyar, F. P. Wathan, and R. Tafazolli. Novel Low-Density Signature for Synchronous CDMA Systems Over AWGN Channel. *IEEE Transactions on Signal Processing*, 56(4):1616–1626, April 2008.
- [14] H. Nikopour and H. Baligh. Sparse code multiple access. In *2013 IEEE 24th Annual International Symposium on Personal, Indoor, and Mobile Radio Communications (PIMRC)*, pages 332–336, Sep. 2013.
- [15] L. Dai, B. Wang, Y. Yuan, S. Han, C. I, and Z. Wang. Non-orthogonal multiple access for 5G: solutions, challenges, opportunities, and future research trends. *IEEE Communications Magazine*, 53(9):74–81, Sep. 2015.
- [16] Arief Hamdani. OFDMA and MIMO. <https://www.slideshare.net/hamdani2/day-one-ofdma-and-mimo>. Accessed:2019-09-13.
- [17] I. Kuo, W. Hu, and T. Chiueh. Limited search sphere decoder and adaptive detector for NOMA with SU-MIMO. In *2016 IEEE Asia Pacific Conference on Circuits and Systems (APCCAS)*, pages 573–576, Oct 2016.

- [18] J. Ketonen, M. Juntti, and J. R. Cavallaro. Performance—Complexity Comparison of Receivers for a LTE MIMO–OFDM System. *IEEE Transactions on Signal Processing*, 58(6):3360–3372, June 2010.
- [19] M. Myllyla, M. Juntti, and J. R. Cavallaro. Implementation Aspects of List Sphere Detector Algorithms. In *IEEE GLOBECOM 2007 - IEEE Global Telecommunications Conference*, pages 3915–3920, Nov 2007.
- [20] M. Myllyla, P. Silvola, M. Juntti, and J. R. Cavallaro. Comparison of Two Novel List Sphere Detector Algorithms for MIMO-OFDM Systems. In *2006 IEEE 17th International Symposium on Personal, Indoor and Mobile Radio Communications*, pages 1–5, Sep. 2006.
- [21] R. El Chall, F. Nouvel, M. H elard, and M. Liu. Low complexity k-best based iterative receiver for MIMO systems. In *2014 6th International Congress on Ultra Modern Telecommunications and Control Systems and Workshops (ICUMT)*, pages 451–455, Oct 2014.
- [22] Ibrahim Bello, Basel Halak, Mohammed El-Hajjar, and Mark Zwolinski. A Survey of VLSI Implementations of Tree Search Algorithms for MIMO Detection. *Circuits, Systems, and Signal Processing*, 35, 12 2015.
- [23] Rada El Chall. Iterative decoder for MIMO-OFDMA based system . Convergence, Performance and Complexity. October 2015.
- [24] Fincke U. and M. Pohst. Improved Methods for Calculating Vectors of Short Length in a Lattice, Including a Complexity Analysis. *Mathematics of Computation*, 44(170):463–471, 1985.
- [25] M. Myllyla, M. Juntti, and J. R. Cavallaro. A List Sphere Detector based on Dijkstra’s Algorithm for MIMO-OFDM Systems. In *2007 IEEE 18th International Symposium on Personal, Indoor and Mobile Radio Communications*, pages 1–5, Sep. 2007.
- [26] V. Kalokidou, O. Johnson, and R. Piechocki. A hybrid TIM-NOMA scheme for the SISO Broadcast Channel. In *2015 IEEE International Conference on Communication Workshop (ICCW)*, pages 387–392, June 2015.

- [27] J. A. Oviedo and H. R. Sadjadpour. A Fair Power Allocation Approach to NOMA in Multiuser SISO Systems. *IEEE Transactions on Vehicular Technology*, 66(9):7974–7985, Sep. 2017.
- [28] T. Manglayev, R. C. Kizilirmak, Y. H. Kho, N. Bazhayev, and I. Lebedev. NOMA with imperfect SIC implementation. In *IEEE EUROCON 2017 -17th International Conference on Smart Technologies*, pages 22–25, July 2017.
- [29] Z. Wu, K. Lu, C. Jiang, and X. Shao. Comprehensive Study and Comparison on 5G NOMA Schemes. *IEEE Access*, 6:18511–18519, 2018.
- [30] 3GPP. Evolved Universal Terrestrial Radio Access (E-UTRA);Physical channels and modulation. Technical Specification (TS) 36.211, 3rd Generation Partnership Project (3GPP), 04 2017. Version 14.2.0.
- [31] www.sharetechnote.com. LTE Quick Reference .
- [32] LTE Advanced - Transmission Mode. https://www.sharetechnote.com/html/LTE_Advanced_TM.html. Accessed:2019-09-10.